

**OPTICAL SIMULATION APPROACH AS A TECHNIQUE TO
DETERMINE THE EFFICIENCY OF ULTRAVIOLET GERMICIDAL
IRRADIATION IN SURFACE DISINFECTANT**

By

LEE WEN ZHE

A thesis submitted to the Department of Mechanical and Material Engineering,
Lee Kong Chian Faculty of Engineering & Science,
Universiti Tunku Abdul Rahman,
in partial fulfillment of the requirements for the degree of
Master of Engineering (Mechanical)
March 2023

ABSTRACT

OPTICAL SIMULATION APPROACH AS A TECHNIQUE TO DETERMINE THE EFFICIENCY OF ULTRAVIOLET GERMICIDAL IRRADIATION IN SURFACE DISINFECTANT

Lee Wen Zhe

The utilization of surface disinfection has gained increased popularity in recent years due to its effectiveness in killing pathogens. Ultraviolet Germicidal Irradiation (UVGI) is preferable as it is more environmentally friendly compared to other methods. In order to maximize the usage of UVGI technology, it is necessary to identify the mechanism and irradiation performance of the UVGI technology. However, most of the paper are using physical approached nowadays to identify the efficiency of UVGI. In this paper, optical simulation approach had been used to investigate the efficiency of ultraviolet C light (UV-C) subjected to the power of light source and distance from light source based on direct ray tracing light simulation methods at a fixed spectrum of 254 nm. A sample of SARS-Cov-2 had been selected to go through surface disinfection for 3, 4 and 5 log reduction respectively. The efficiency of the UVGI technology is further discussed based on the required exposure time to reach total dose for the surface disinfection. According to the simulation, the efficiency of the UVGI system decreases as the distance from the light source increases. However, the result might be varying based on the power of light source.

ACKNOWLEDGEMENT

First and foremost, I want to thank Dr. Jaslyn Low Foon Siang, my project supervisor for her patience and never-ending support and guidance throughout this project. This project would not be possible without her guidance. I would also like to express my appreciation to Universiti Tunku Abdul Rahman (UTAR), Lee Kong Chian Faculty of Engineering & Science (LKCFES) for creating a platform for me to test myself and my abilities that I have obtained through the journey in Mechanical Engineering. Lastly, I uphold my sincere gratitude to my family who has provided much encouragement, motivation, and support to me.

APPROVAL SHEET

This dissertation/thesis entitled “OPTICAL SIMULATION APPROACH AS A TECHNIQUE TO DETERMINE THE EFFICIENCY OF ULTRAVIOLET GERMICIDAL IRRADIATION IN SURFACE DISINFECTANT” was prepared by LEE WEN ZHE and submitted as partial fulfillment of the requirements for the degree of Master of Engineering in Mechanical at Universiti Tunku Abdul Rahman.

Approved by:



(Dr. Jaslyn Low Foon Siang)

Date: 12 April 2023

Department of Mechanical and Material Engineering
Lee Kong Chian Faculty of Engineering & Science
Universiti Tunku Abdul Rahman

SUBMISSION SHEET

**LEE KONG CHIAN FACULTY OF ENGINEERING & SCIENCE
UNIVERSITI TUNKU ABDUL RAHMAN**

Date: 12 APR 2023

SUBMISSION OF FINAL YEAR PROJECT /DISSERTATION/THESIS

It is hereby certified that LEE WEN ZHE (ID No: 2102683) has completed this thesis entitled OPTICAL SIMULATION APPROACH AS A TECHNIQUE TO DETERMINE THE EFFICIENCY OF ULTRAVIOLET GERMICIDAL IRRADIATION IN SURFACE DISINFECTANT under the supervision of Dr. Jaslyn Low Foon Siang from the Department of Mechanical and Material Engineering, Lee Kong Chian Faculty of Engineering & Science.

I understand that University will upload softcopy of my thesis in pdf format into UTAR Institutional Repository, which may be made accessible to UTAR community and public.

Yours truly,

LEE WEN ZHE

DECLARATION

I hereby declare that the dissertation is based on my original work except for quotations and citations which have been duly acknowledged. I also declare that it has not been previously or concurrently submitted for any other degree at UTAR or other institutions.

Name: LEE WEN ZHE

Date: 12 April 2023

TABLE OF CONTENTS

Contents

ABSTRACT	ii
ACKNOWLEDGEMENT	iii
APPROVAL SHEET	iv
SUBMISSION SHEET	v
DECLARATION.....	vi
TABLE OF CONTENTS	vii
LIST OF TABLES.....	ix
LIST OF FIGURES	xi
LIST OF ABBREVIATIONS	xvii
INTRODUCTION.....	1
1.1 Research Background	1
1.2 Problem Statement	2
1.3 Research Objectives	3
1.4 Research Scope	3
1.5 Research Contribution	4
LITERATURE REVIEW	5
2.2 Factors Impacting UVGI Efficacy	8
2.2.1 Length of Exposure	9
2.2.2 Distance from Source to Surface	10
2.2.3 Intensity of Source	11
2.3 UVGI Technologies	12
2.3.1 Mercury Lamps	13
2.3.2 Pulsed Lamps	14
2.3.3 UV-Light Emitting Diodes	16
2.4 Application of UVGI Technology as Surface Disinfectant	18
2.5 Approach in Identifying UVGI Dose	22
2.5.1 Contact Plate Method	22
2.5.2 Swab Method	24
2.5.3 Other Physical Sampling Method	25
2.5.4 Computational Fluid Dynamics (CFD)	26
2.5.5 Optical Simulation Approach	26
2.6 Log Reduction Value for Disinfection	27
2.7 Summary	30
METHODOLOGY.....	31
3.1 Project Process Flow	31
3.2 Gantt Chart	32
3.3 Identify Case Study	33

3.4	Creation and Setup of Model	36
3.5	Identification of Exposure Time to Achieve Optimal Dose	39
RESULTS AND DISCUSSION.....		40
4.1	ANSYS SPEOS Results for 36 W Light Source at Vertical Setup	40
4.2	ANSYS SPEOS Results for 55 W Light Source at Vertical Setup	48
4.3	ANSYS SPEOS Results for 36 W Light Source at Angled Setup	56
4.4	ANSYS SPEOS Results for 55 W Light Source at Angled Setup	64
4.5	Post-Process of Result	72
CONCLUSIONS		84
5.1	Summary	84
REFERENCES		86
APPENDICES.....		96

LIST OF TABLES

Table		Page
2.1	Percentage of Reduction subject to Log Reduction	28
2.2	Dose Required for Different Log Reduction Value	29
2.3	Dose Required for Disinfectant for SARS-Cov-2	29
4.1	Average Irradiation versus Distance at different Power Source for Vertical Setup	73
4.2	Average Irradiation versus Distance at different Power Source for Angled Setup	74
4.3	Total Required Exposure Time Required to Reach 3 LRV for Vertical Configuration	76
4.4	Total Required Exposure Time Required to Reach 4 LRV for Vertical Configuration	76
4.5	Total Required Exposure Time Required to Reach 5 LRV for Vertical Configuration	77
4.6	Total Required Exposure Time Required to Reach 3 LRV for Angled Configuration	79
4.7	Total Required Exposure Time Required to Reach 4 LRV for Angled Configuration	79
4.8	Total Required Exposure Time Required to Reach 5 LRV for Angled Configuration	79

4.9	Summary of Total Exposure Time Required to Reach Respective LRV for 36W Vertical Configuration	82
4.10	Summary of Total Exposure Time Required to Reach Respective LRV for 55W Vertical Configuration	82
4.11	Summary of Total Exposure Time Required to Reach Respective LRV for 36W Angled Configuration	83
4.12	Summary of Total Exposure Time Required to Reach Respective LRV for 36W Angled Configuration	83

LIST OF FIGURES

Figures	Page
2.1 Wavelength at Different Light Spectrums	6
2.2 Pathogens Reduction Rate versus Exposure Time	9
2.3 Irradiance Distribution versus Distance	10
2.4 Working Mechanism of Mercury Lamp	14
2.5 Spectrum Generated by Mercury Lamp	14
2.6 Structure of Pulsed Lamp	15
2.7 Spectrum Generated by Pulsed Lamp	16
2.8 Structure of UV-Light Emitting Diodes	17
2.9 Spectrum Generated by UV-Light Emitting Diodes	17
2.10 Survival Rate versus Exposure Time	19
2.11 Illustration of Robot Hovering UV Flashlight	21
2.12 Procedure to Conduct Contact Plate Method	23
2.13 Recommended Procedure to Conduct Swab Method	24
3.1 Project Flow Chart	31
3.2 Project Gantt Chart (1)	32
3.3 Project Gantt Chart (2)	32
3.4 Dimension of Bulb Label	34
3.5 Illustration of the Light Bulb	34
3.6 Specification of the Sensor	35
3.7 Sample of 3D Model for Vertical Setup	36
3.8 Sample of 3D Model for Angled Setup	37

3.9	Sample Simulation Setting for Vertical Setup	38
3.10	Sample Simulation Setting for Angled Setup	38
4.1	Irradiation Profile at 10 mm	40
4.2	Irradiation Profile at 30 mm	41
4.3	Irradiation Profile at 50 mm	41
4.4	Irradiation Profile at 70 mm	42
4.5	Irradiation Profile at 90 mm	42
4.6	Irradiation Profile at 110 mm	43
4.7	Irradiation Profile at 130 mm	43
4.8	Irradiation Profile at 150 mm	44
4.9	Irradiation Profile at 170 mm	44
4.10	Irradiation Profile at 190 mm	45
4.11	Irradiation Profile at 210 mm	45
4.12	Average irradiation obtained by sensor at 10 mm	46
4.13	Average irradiation obtained by sensor at 30 mm	46
4.14	Average irradiation obtained by sensor at 50 mm	46
4.15	Average irradiation obtained by sensor at 70 mm	46
4.16	Average irradiation obtained by sensor at 90 mm	46
4.17	Average irradiation obtained by sensor at 110 mm	46
4.18	Average irradiation obtained by sensor at 130 mm	47
4.19	Average irradiation obtained by sensor at 150 mm	47
4.20	Average irradiation obtained by sensor at 170 mm	47
4.21	Average irradiation obtained by sensor at 190 mm	47
4.22	Average irradiation obtained by sensor at 210 mm	47
4.23	Irradiation Profile at 10 mm	48

4.24	Irradiation Profile at 30 mm	49
4.25	Irradiation Profile at 50 mm	49
4.26	Irradiation Profile at 70 mm	50
4.27	Irradiation Profile at 90 mm	50
4.28	Irradiation Profile at 110 mm	51
4.29	Irradiation Profile at 130 mm	51
4.30	Irradiation Profile at 150 mm	52
4.31	Irradiation Profile at 170 mm	52
4.32	Irradiation Profile at 190 mm	53
4.33	Irradiation Profile at 210 mm	53
4.34	Average irradiation obtained by sensor at 10 mm	54
4.35	Average irradiation obtained by sensor at 30 mm	54
4.36	Average irradiation obtained by sensor at 50 mm	54
4.37	Average irradiation obtained by sensor at 70 mm	54
4.38	Average irradiation obtained by sensor at 90 mm	54
4.39	Average irradiation obtained by sensor at 110 mm	54
4.40	Average irradiation obtained by sensor at 130 mm	55
4.41	Average irradiation obtained by sensor at 150 mm	55
4.42	Average irradiation obtained by sensor at 170 mm	55
4.43	Average irradiation obtained by sensor at 190 mm	55
4.44	Average irradiation obtained by sensor at 210 mm	55
4.45	Irradiation Profile at 10 mm	56
4.46	Irradiation Profile at 30 mm	57
4.47	Irradiation Profile at 50 mm	57
4.48	Irradiation Profile at 70 mm	58

4.49	Irradiation Profile at 90 mm	58
4.50	Irradiation Profile at 110 mm	59
4.51	Irradiation Profile at 130 mm	59
4.52	Irradiation Profile at 150 mm	60
4.53	Irradiation Profile at 170 mm	60
4.54	Irradiation Profile at 190 mm	61
4.55	Irradiation Profile at 210 mm	61
4.56	Average irradiation obtained by sensor at 10 mm	62
4.57	Average irradiation obtained by sensor at 30 mm	62
4.58	Average irradiation obtained by sensor at 50 mm	62
4.59	Average irradiation obtained by sensor at 70 mm	62
4.60	Average irradiation obtained by sensor at 90 mm	62
4.61	Average irradiation obtained by sensor at 110 mm	62
4.62	Average irradiation obtained by sensor at 130 mm	63
4.63	Average irradiation obtained by sensor at 150 mm	63
4.64	Average irradiation obtained by sensor at 170 mm	63
4.65	Average irradiation obtained by sensor at 190 mm	63
4.66	Average irradiation obtained by sensor at 210 mm	63
4.67	Irradiation Profile at 10 mm	64
4.68	Irradiation Profile at 30 mm	65
4.69	Irradiation Profile at 50 mm	65
4.70	Irradiation Profile at 70 mm	66
4.71	Irradiation Profile at 90 mm	66
4.72	Irradiation Profile at 110 mm	67
4.73	Irradiation Profile at 130 mm	67

4.74	Irradiation Profile at 150 mm	68
4.75	Irradiation Profile at 170 mm	68
4.76	Irradiation Profile at 190 mm	69
4.77	Irradiation Profile at 210 mm	69
4.78	Average irradiation obtained by sensor at 10 mm	70
4.79	Average irradiation obtained by sensor at 30 mm	70
4.80	Average irradiation obtained by sensor at 50 mm	70
4.81	Average irradiation obtained by sensor at 70 mm	70
4.82	Average irradiation obtained by sensor at 90 mm	70
4.83	Average irradiation obtained by sensor at 110 mm	70
4.84	Average irradiation obtained by sensor at 130 mm	71
4.85	Average irradiation obtained by sensor at 150 mm	71
4.86	Average irradiation obtained by sensor at 170 mm	71
4.87	Average irradiation obtained by sensor at 190 mm	71
4.88	Average irradiation obtained by sensor at 210 mm	71
4.89	Average Irradiation versus Distance at different Power Source for Vertical Setup	73
4.90	Average Irradiation versus Distance at different Power Source for Angled Setup	74
4.91	Total Required Exposure Time Required to Reach 3 LRV for Vertical Configuration	77
4.92	Total Required Exposure Time Required to Reach 4 LRV for Vertical Configuration	78
4.93	Total Required Exposure Time Required to Reach 5 LRV for Vertical Configuration	78

4.94	Total Required Exposure Time Required to Reach 3	
	LRV for Angled Configuration	80
4.95	Total Required Exposure Time Required to Reach 4	
	LRV for Angled Configuration	80
4.96	Total Required Exposure Time Required to Reach 5	
	LRV for Angled Configuration	81

LIST OF ABBREVIATIONS

ASHRAE	The American Society of Heating, Refrigerating and Air-Conditioning Engineers
CFD	Computational Fluid Dynamics
DNA	Deoxyribonucleic acid
GCRTA	Greater Cleveland Regional Transit Authority
HVAC	Heating, Ventilation and Air-Conditioning Systems
LEDs	Light emitting diodes
LPM	Low-pressure mercury
LRV	Log Reduction Value
MPM	Medium-pressure mercury
MTA	New York Metropolitan Transportation Authority
NCTD	North County Transit District

PBS	Phosphate-buffered saline
RODAC	Replicate Organism Detection and Counting
TSA	Tryptone Soya Agar
UV	Ultraviolet
UV-C	Ultraviolet C
UVGI	Ultraviolet germicidal irradiation

CHAPTER 1

INTRODUCTION

1.1 Research Background

Surface disinfection takes a significant part in transmissible disease outbreaks as it demolishes or inactivates the pathogenic microorganisms on an inert surface. Disinfectant commonly refers to an approach or a substance that used to cut down the microbial contamination to acceptable level based on public health standpoint. Generally, infection inhibition can be done by both physical and chemical means (Ghedini et al., 2021). The typical substances to use as disinfectant can be classified into alcohols, halogens, peroxygens, quaternary ammonium compounds, ozone as well as ultraviolet (UV). However, some of the chemical substances will cause damage and degradation to the applied surfaces and cause some diseases if not handled properly. For instance, continued exposure of hydrogen peroxide may cause organ failure, fatal septic shock and collapse of redox homeostasis (Pravda, 2020). Thus, ultraviolet C (UV-C) light application has been implemented as one of relatively safer disinfectant as it is eco-friendly with no residue characteristic (Artasensi et al., 2021). UV-C is further investigated and use in ultraviolet germicidal irradiation (UVGI) with a wavelength of 254 nm to inactivate or kill pathogens by destroying their deoxyribonucleic acid (DNA) (Yamano et al., 2020). However, the efficacy of this method is highly depending on several criteria such as intensity and dose of the UV

light, organic load and pathogen, exposure time, distance from device as well as whether the surface to be cleaned is within direct line-of sight (Elgужja et al., 2019), (Jones et al., 2020). This paper aims to highlight the efficiency of UVGI in surface disinfection by optical simulation approach as it is able to provide a visualization regarding performance of UVGI technologies in the early stage of study and designing.

1.2 Problem Statement

The inactivation of pathogens on surfaces may not be effective due to several factors such as power of UV light source as well as distance from the UV light source. These area with low dose creates a need to increase the exposure time to provide effective inactivation of pathogen microorganism. In order to determine those significant area, most of the paper are using physical equipment to collect the data via trial and error of different combination of time and radiation intensity (Zakaria et al., 2016). This method is straightforward however it might take lots of effort and time. Thus, optical simulation approach had been introduced to simulate radiation intensity to eliminate the trial-and-error process and at the same time, to identify the efficacy of UVGI technology subject to the power and distance.

1.3 Research Objectives

- a) To conduct simulation using optical approach to test different combinations of distance and radiation intensity of UVGI light sources of 254nm
- b) To evaluate the efficiency of UVGI for surface disinfectants
- c) To propose optimal dose of UVGI for surface disinfectants

1.4 Research Scope

In this project, various of literature reviews will be conducted to identify the necessary dose for surface disinfection. Several 3D models will be generated in ANSYS software to represent the light source and sensor. Next, the irradiation performance between different power of light source and distance from the light source are determined by running an optical simulation in ANSYS SPEOS software. In actual case, although the inactivation of viruses on surfaces may not be effective due to blocking of UV radiation when the bulb is covered with dust, however, this project will assume that the bulb is just cleaned and used for the surface disinfection. Thus, the direct ray from the light source will be considered during the optical simulation. The results will illustrate the irradiation performance and used to determine the efficiency of UV-C light at different condition.

1.5 Research Contribution

The findings in this study will help the engineers to design a surface disinfection system with proper setup and requirement that could satisfy different purpose via optical simulation approach. The optical simulation approach helps to reduce the trial-and-error process and in other words, reduces the resources needed for multiple physical testing. In addition, the findings also help to improve the engineer knowledge on UVGI efficacy as well as provide a standard guideline for them to determine efficacy of UVGI through optimal simulation approach. Thus, this will allow engineers to complete the design process in a shorter timeframe.

CHAPTER 2

LITERATURE REVIEW

2.1 Historical Background of Ultraviolet Germicidal Irradiation

Ultraviolet germicidal irradiation (UVGI) is defined as the utilization of ultraviolet (UV) energy to destroy bacterial, viral and fungal organisms in order to prevent the spread of infectious diseases. The history of UVGI can be traced back to 1877, when Downes and Blunt founded that the growth of microorganisms can be prevented by the exposure of sunlight (Downes and Blunt, 1877). In the same experiment, they also observed that the inactivation of microbial growth was impacted by the exposure time, intensity, and wavelength (Downes and Blunt, 1879). In 1878 and 1881, Tyndall published two papers that support the results proposed by Downes and Blunt, which also raise the concept that a shorter wavelength of the solar spectrum might results in a better inactivation of microbial growth (Tyndall, 1878), (Tyndall, 1881).

In the following year, more studies were conducted to determine and identify the specific wavelengths of light that contributed to inactivation of microbial growth, and the study can be further classified into several light spectrum such as UV-C light (200 -280 nm), UV-B light (280 -315 nm), UV-A light (315 -400 nm), visible light (400- 700 nm) and infrared light

(O'Connor et al., 2020), (Kohli et al., 2019). Figure 2.1 indicates the illustration of wavelength at different light spectrums.

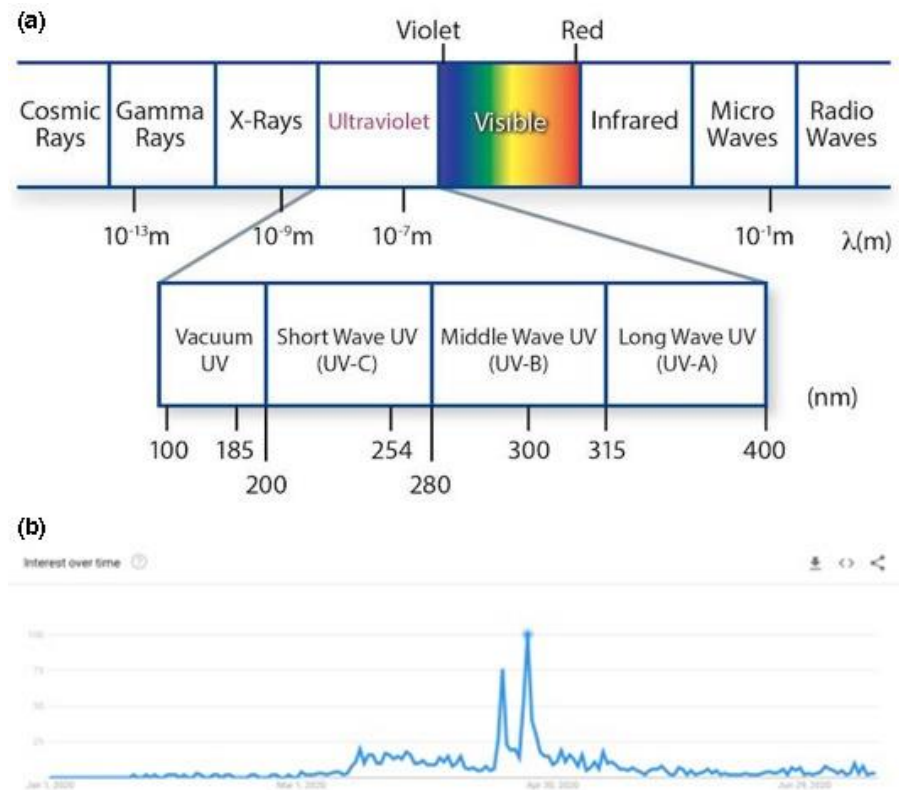


Figure 2.1: Wavelength at Different Light Spectrums

(O'Connor et al., 2020)

In 1890, Koch claimed that different types of microorganism might require different amounts of doses for the same level of inactivation. He also proved that the lethal effect of sunlight on microorganism and the concept was further expanded by Geisler in 1892. In his study, Geisler claimed that a shorter wavelength of light is more efficient in destroying microorganism compared to a longer wavelength radiation. In addition, he also stated that lethal effects of longer wavelength radiation were amplified at increased intensities. In term of infrared radiation, Buchner proved that infrared

radiation does not have much contribution on germicidal action of sunlight by passing it through an infrared-absorbing water filter before it reached the microorganism sample (Kowalski, 2009). In 1901 and 1903, Bang claimed that UV-B and UV-C radiation possess a higher efficiency compared to UV-A in inactivation of microbial growth (Hockberger, 2007). Moreover, in 1903, Barnard and Morgan provided a more comprehensive results that peak bactericidal effectiveness occurred at a wavelength between 226.5 nm and 328.7 nm (Bernard & Morgan, 1904). This was a major finding that allowed other researcher to locate the area of study related to germicidal wavelength. Moreover, Hertel conducted a quantitative analysis using thermoelectric measurement approach with prism to describe the relative intensity of the light emitted by an arc lamp in 1904 and 1905. This data was further used to predict the level of germicidal effectiveness in different light spectrum. The results indicated that UV-C possesses the highest effectiveness, followed by UV-B, and UV-A. However, the visible radiation has the lowest effectiveness for germicidal purpose (Walton, 1916). In other word, the dose needed to destroy the microorganism increased as the wavelength of light increased. This study concluded that UV-C is the most suitable light spectrum to be selected for microbial inactivation.

The number of studies related to UVGI had increased tremendously after the determination of UV-C as inactivation spectrum. In 1914, the mutagenic effects of UVGI were discovered by Henri. He observed the modification on the metabolism when the bacteria exposed to a certain doses of UV radiation (Enwemeka et al., 2021). In addition, a first analytical bactericidal

action spectrum had been published by Gates in 1930. He claimed that the most effective light spectrum for inactivation of microbial growth is 265 nm. In his paper, he stated that the cell destroys due to the alternation of genetic material instead of protein (Gates, 1930). This point of view was further proved by other researchers and become the major view in UVGI research area. For instance, Beukers & Berends, as well as Coohill had discussed the biological effects of UV radiation on microorganisms in their paper in 1960 and 1997 (Beukers & Berends, 1960); (Coohill, 1997).

In short, UVGI is one of the common methodologies to inactivate microbial growth by damaging mutagenic component in the cell. The interest towards UVGI technology grow tremendously around 1980s and the current papers are more interested and focused on the efficacy of UVGI technology.

2.2 Factors Impacting UVGI Efficacy

The efficacy of UVGI is depending on several factors. Based on The American Society of Heating, Refrigerating and Air-Conditioning Engineers (ASHRAE) handbook, it stated that the factors that impact the radiant energy levels to a surface are length of exposure, distance from source to surface as well as the intensity of source (Kennedy, 2019).

2.2.1 Length of Exposure

The length of exposure is referred to how long the pathogens are exposed to the UVGI device. In general, the inactivation effect of UVGI device will be greater at a longer exposure time. In 2019, Yang J et al conducted an experiment by designing several UVGI system with fixed distance and different exposure time. In this experiment, he observed the reduction rate of pathogens and concluded that the system will have a higher efficacy at a longer exposure time (Yang et al., 2019). Figure 2.2 indicates one of the tabulated results from the paper regarding relation between reduction rate of pathogens and exposure time.

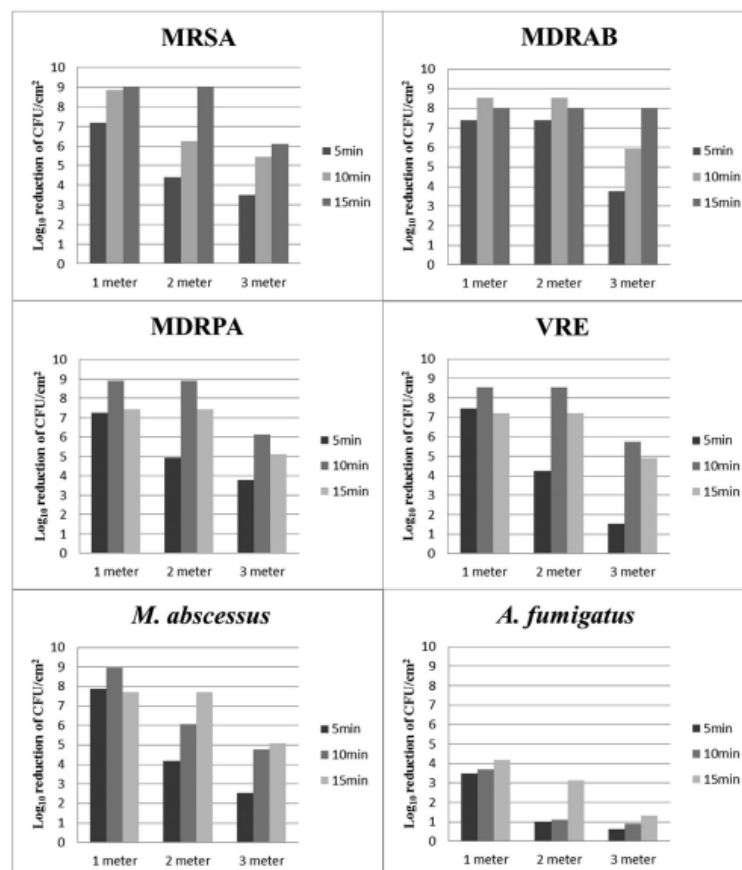


Figure 2.2: Pathogens Reduction Rate versus Exposure Time

(Yang et al., 2019)

In addition, Fredes et al. had discussed the contribution of exposure time towards the dose in his study in 2021. This study proved that length of exposure is one of the key factors that impact the efficacy of UVGI (Fredes et al., 2021).

2.2.2 Distance from Source to Surface

Shadowing effect due to the distance between source and surface acted as another key factor to determine the efficacy of UVGI. In general, the inactivation effect of UVGI device will be greater at a shorter radiated distance. In the study conducted by Fredes et al., they had investigated into the relation between the distance and the exposure time and concluded that the average irradiance decreased as the distance between source and surface increased (Fredes et al., 2021). Figure 2.3 indicates one of the tabulated graphs that represent the relation between irradiance distribution and distance from light source in their study.

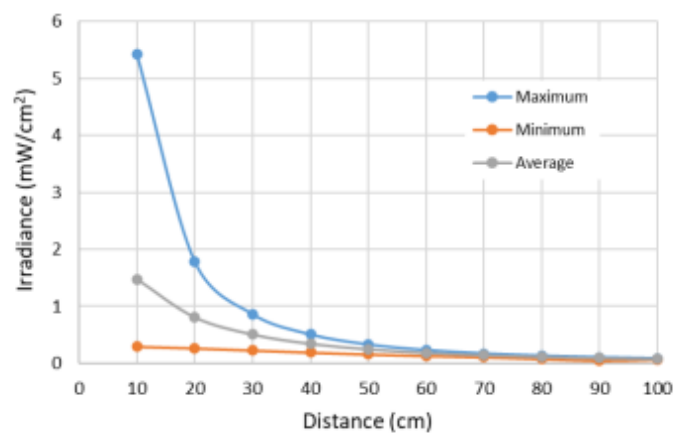


Figure 2.3: Irradiance Distribution versus Distance

(Fredes et al., 2021)

Furthermore, Yang J et al also claimed that the same behavior occurred in his study whereas a higher efficacy happened at a shorter distance from the source (Yang et al., 2019). The same behavior also observed in the experiment conducted by Wan Yunoh et al. in 2021 (Wan Yunoh et al., 2021).

2.2.3 Intensity of Source

The efficacy of the UVGI system also impacted by the performance of the source. Some physical factors that might influence the performance are air temperature and air humidity. Therefore, commonly the equipment manufacturers will provide the data of expected intensity of equipment at a given distance along with some correction factor. Those correction are used to improve the accuracy of prediction during calculation of dose received by the target surface (Luo & Zhong, 2021).

Relative Humidity (RH) is referred to the ratio of water vapor present in the air at certain temperature. It is founded that RH possesses a mixed influence on UV sensitivity in the history. For instance, Lidwell and Lowbury stated that the decay rate for microorganism decreased with an increased RH in 1950 (Lidwell & Lowbury, 1950). However, Philips had claimed that increased Rh will decrease the decay rate under UVGI exposure in 1985 (Philips, 1985). Based on the finding, the results suggested that there is certain relationship between the RH and UVGI sensitivity for different type

of microorganism. This view was further supported by Hao in 2021 due to the mixed influence reported in the literature (Luo & Zhong, 2021).

Although air temperature might impact the power output of UVGI equipment if it exceeds the design parameters, some study shows that there is certain relation between air temperature with the lamp irradiance. For example, in 2020, Zhang et al. observed that the lamp irradiance shows an increasing and then decreasing trend when the air temperature increases from 20.5 to 25.5 (Zhang et al., 2020). However, Lau founded an opposite trend when he increases the air temperature from 15.5 to 25.5 (Lau et al., 2009). Both experiments are conducted under constant air velocity of 3 m/s. The difference between the results might be due to the different design approach of the UVGI equipment. Therefore, data from manufacturer should be consulted to determine the actual performance for each of the UVGI equipment.

2.3 UVGI Technologies

UVGI equipment requires a source to generate light which either by ionization or excitation means. The performance of UVGI depends on the correct matching of the source parameter to the demand of UVGI application. There are three major types of UVGI technology, named as mercury lamp, pulsed lamp as well as Far-UV (Scott et al., 2022).

2.3.1 Mercury Lamps

Mercury lamp is a device that filled by vapor mercury and starting gas such as argon gas. It can be further categorized into low-pressure mercury (LPM) and medium-pressure mercury (MPM) lamp based on the operating mercury vapor pressure. Once the mercury vapor is excited in an electric field, it generates different narrow-band germicidal irradiation. For instance, LPM that operates around 102 Pa at 40 degrees Celsius will generate two spectrums at 185 nm and 253.7 nm. The 185 nm spectrum is responsible for ozone production; thus, a soft glass will normally be used to eliminate this ozone-forming irradiance. The 253.7 nm spectrum is out of ozone producing region and is very useful for germicidal purpose (Raggi et al., 2018); (Scott et al., 2022).

On the other hand, MPM operates around 105 Pa and possesses a temperature up to 800 degrees Celsius in a stable operation. It generates several spectra from 250 nm to 600 nm, which cover the spectrum from ultraviolet light to visible light range (Cutler & Zimmerman, 2011). This strong radiation flux results in high penetration depth which is possible to use for certain food processing application such as photo-degradation and oxidation due to its high penetration depth. However, it is not suitable to use for germicidal purpose (Kennedy, 2019). Figures 2.4 and 2.5 illustrate the working mechanism and spectrum generated by mercury lamp.

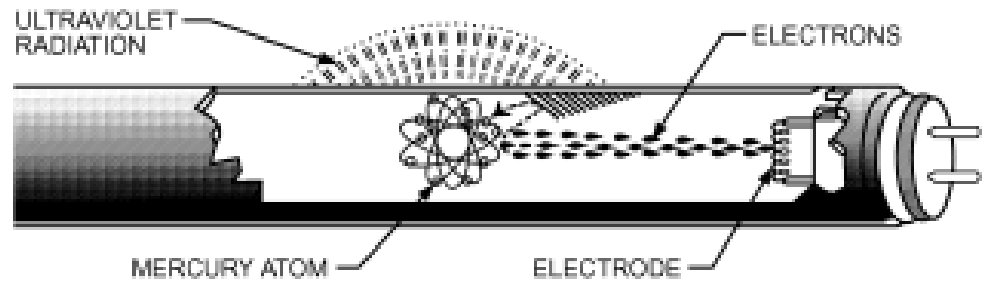


Figure 2.4: Working Mechanism of Mercury Lamp (Kennedy, 2019)

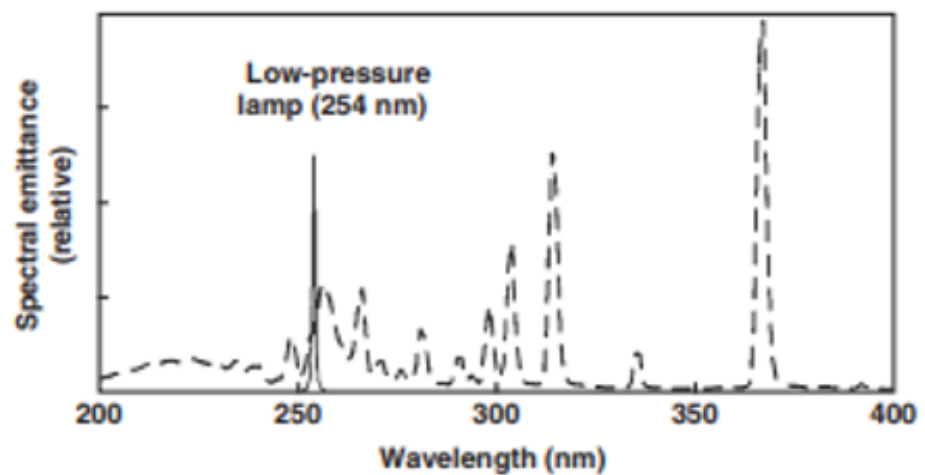


Figure 2.5: Spectrum Generated by Mercury Lamp

(Cutler & Zimmerman, 2011)

2.3.2 Pulsed Lamps

Pulsed lamp is an alternative device that utilize the xenon light to generate high energy pulse with wider spectrum and short duration of exposure to achieve germicidal purpose. In pulsed lamp, the stored alternating current is discharged through a switch control to generate pulse in a time interval of 100 ms. It possesses a higher efficacy compared to mercury lamp due to its broader spectrum and greater intensity (Scott et al., 2022). Thus, pulsed

lamp has the potential to deliver higher spectrum which provide enhanced treatment rates as well as penetrate opaque fluids better than mercury lamp (Mallikarjuna et al., 2016); (Song et al., 2020). In 2015, Jinadatha et al. had claimed that the efficacy of pulsed lamp to reduce the level of known microorganism is higher compared to standard manual room terminal cleaning procedure (Jinadatha et al., 2015). This viewpoint was also supported by Haddad et al. in 2017 (El Haddad et al., 2017). Figures 2.6 and 2.7 indicate the structure and spectrum generated by pulsed lamp.

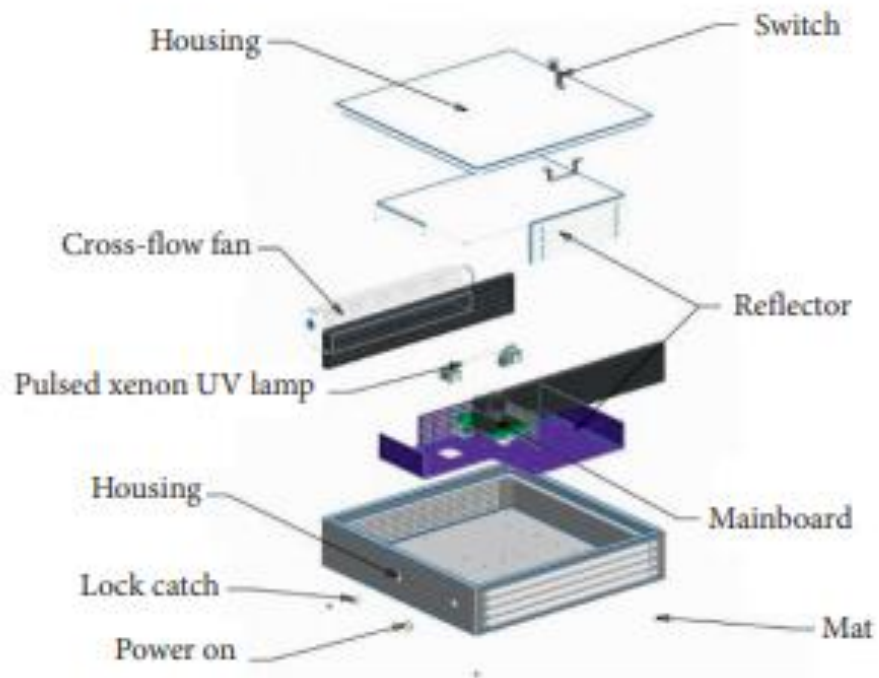


Figure 2.6: Structure of Pulsed Lamp (Song et al., 2020)

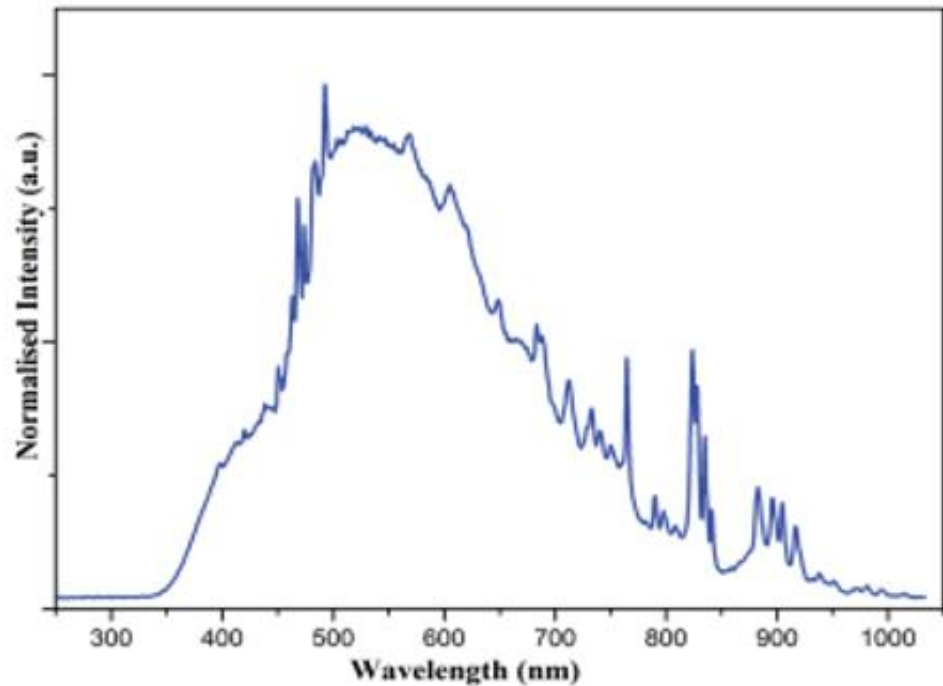


Figure 2.7: Spectrum Generated by Pulsed Lamp

(Mallikarjuna et al., 2016)

2.3.3 UV-Light Emitting Diodes

UV-light emitting diodes (LEDs) are semiconductor that emit light when photon is generated by a combination between carriers from different polarities. The wavelength of the photon is determined by the energy difference between each energy level. This device possesses several advantages such as having a long lifespan, energy-efficient and do not contain mercury component (Scott et al., 2022). Generally, the wavelength of this device falls between 240 – 400 nm. One of the examples of LEDs are the device formed by gallium nitride, aluminum nitride as well as intermediate alloys. In fact, most of the study related to bacteria claimed that a higher UV rate constants were founded in UV-LED system compared to

other conventional UVGI system. This can be further explained by most of microorganisms has a peak absorption between 260 nm and 270 nm (Sholtes et al., 2016); (Song et al., 2019). Figures 2.8 and 2.9 illustrate the structure and spectrum generated by UV-LEDs system.

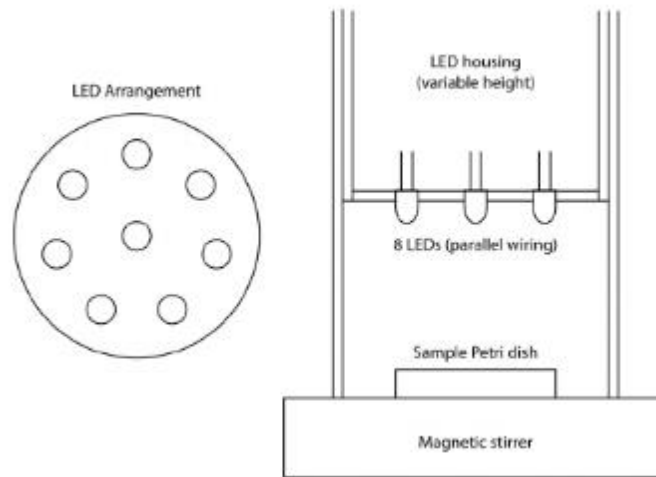


Figure 2.8: Structure of UV-Light Emitting Diodes
(Sholtes et al., 2016)

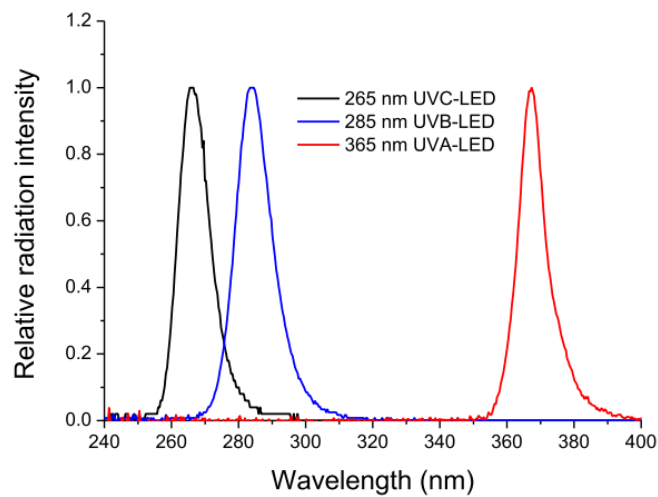


Fig. 1. Emission spectra of 265 nm UVC-LED, 285 nm UVB-LED and 365 nm UVA-LED.

Figure 2.9: Spectrum Generated by UV-Light Emitting Diodes
(Song et al., 2019)

2.4 Application of UVGI Technology as Surface Disinfectant

UVGI had a wide application in different industry. For example, it is implemented as upper-room air lamps or in duct UVGI system to provide air disinfection in Heating, Ventilation and Air-Conditioning Systems (HVAC) industry (Kennedy, 2019). In addition, it also can be used for modifying the structural characteristic of N95 respirator filtration performance in healthcare industry. However, the main application of UVGI is surface disinfection (Lindsley et al., 2015). The application of UVGI in surface disinfections will be discussed in this subtopic.

In agriculture industry, UVGI is designed as handheld UVC lamp and used for disinfection of vegetative or spore forming bacterium. In 2017, Byrns et al. conducted an experiment to determine the efficacy of handheld UVC lamp based on various variable such as air humidity, surface dryness and distance from source. He founded that all the factors contribute to the efficacy of disinfection and the output from handheld UVC lamp is not stable at the initial stage, which will result in loss of 30% intensity over a period of 30 minutes. However, the output is ready to use after 30 minutes (Byrns et al., 2017). Next, Gaya et al. also reviewed the decontamination of vegetables and fresh fruits in her article, with numerous data of optimum UV light conditions to be used for disinfection (Gayas et al., 2019). In 2022, Veerachandra further provided the data of optimum UV light conditions and discuss the effect of UV light on the quality of the vegetables and fresh fruits (Yemmireddy et al., 2022).

In the extend of veterinary industry, Farhad had suggested that UVGI technology can be used in animal husbandry areas for surface disinfection. However, precaution needs to be taken as it will cause harm to acutely exposed mammalian skin (Memarzadeh, 2021). The suggestion had been supported by Wladyslaw in 2021 when he further discussed some common microorganism in human and animal disease. In the study, he provided the test results of UVGI inactivation reduction percentage with respect to time. He further suggested to implement UVGI technology in more veterinary facilities such as kennels and permanent pet housing facilities. These data proved that UVGI is reliable to use in veterinary industry (Wladyslaw, 2021). Figure 2.10 indicates the survival rate of different microbes with respect to time under exposure to UVGI system.

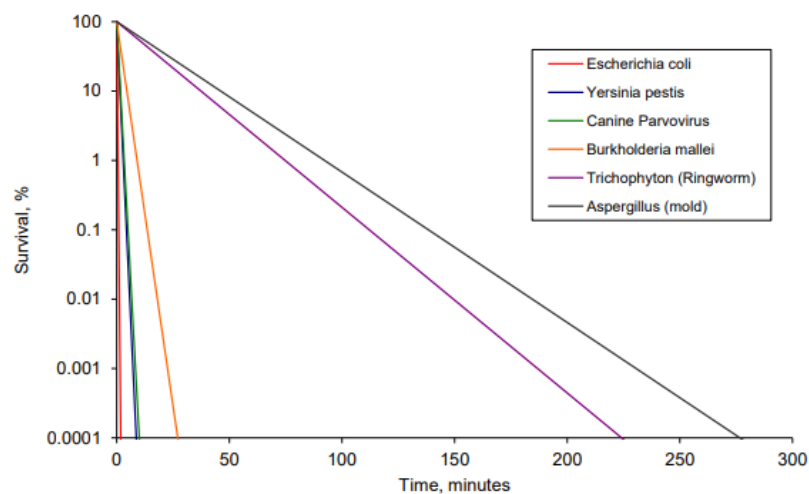


Figure 2.10: Survival Rate versus Exposure Time

(Wladyslaw, 2021)

Furthermore, UVGI is getting more common in the daily life of a consumer. In 2021, Palakornkitti et al. had conducted a study regarding the efficacy of surface disinfection on different type of commercial household ultraviolet C germicidal devices in Thailand. He concluded that most of the devices provide adequate UVC dosage, however certain handheld UVGI disinfection equipment provided a minimum sufficient level of UVC irradiance (Palakornkitti et al., 2021). In addition, Macdufe also discussed the radiometric performance and safety measurements of selected commercial UVGI handheld-type devices and chamber-type devices (Mkabela, 2019). This study indicated that UVGI technology is becoming more and more common in commercial industry.

Moreover, UVGI technology for surface disinfection is widely used in medical industry. For instance, Lindsley et al. had discussed the relation of efficacy with the surface reflectivity. In the paper, he pointed out the effect of the amount of irradiation delivered to different surface are different and highly depends on the reflectivity (Lindsley et al., 2017). In 2021, McGinn et al. claimed that UVGI technology possesses a potential to breakthrough most of the practical limitations of chemical-based approaches disinfection (McGinn et al., 2021). Moreover, the application in medical industry also started to combine with automation, as in 2022, Sanchez and Smart suggested to implement robot with the UVGI technology as human operator might conduct some mistake or error during surface disinfection process. They further verified the efficacy of UVGI on a mobile manipulation robot

(Sanchez & Smart, 2022). Figure 2.11 illustrates the process of robot hovering UV flashlight in an experiment.



Figure 2.11: Illustration of Robot Hovering UV Flashlight

(Sanchez & Smart, 2022)

Lastly, UVGI technology has also been started to use in transport industry in certain country. For example, New York Metropolitan Transportation Authority (MTA), IndyGo, North County Transit District (NCTD) and Greater Cleveland Regional Transit Authority (GCRTA) had started to implement UVGI surface disinfection for interior surface disinfection. On the other hand, similar technology also had been used in Russia to disinfect transit vehicles and facilities. In the document provided by International Association of Public Transport (UITP), the organization mentioned that

Shanghai bus had implement UVGI technology to disinfect the public buses and train carriages.

2.5 Approach in Identifying UVGI Dose

The previous session concluded that the microbial activity will be reduced after expose to certain amount of UVC light. In fact, there are several methods used to measure the reliability of microbial reduction such as contact plates and swabs approach. Some of the other uncommon physical sampling methods were founded and will be recorded in this session (Scott et al., 2022). On the other hand, Computational Fluid Dynamics (CFD) approach and optical analysis approach are also commonly founded in the latest trend to use as a virtual method to investigate case study related to UVGI. Both of the method will be discussed in this section as well.

2.5.1 Contact Plate Method

Contact plate, also known as Replicate Organism Detection And Counting (RODAC) plates, is one of the common approach to use in UVGI sampling surfaces. It is not limited to use in flat surfaces only. However, it is suitable to use on certain curved surfaces, which referred to roll plate method. In this approach, a standard medium will be poured into the contact plate and a force will be applied on the surface to allow microorganisms to stick on the medium (Molitor et al., 2020); (Scott et al., 2022). For instance, Tryptone Soya Agar (TSA) and some other selective agars were used to treat some

specific fungi and bacteria based on their nature. In this approach, the bioburden is quantified after certain period (normally one to two day) by measuring the number of colonies forming units (CFUs) of aerobic incubation at certain temperature (Armellino et al., 2019). In 2021, McGinn and Morikane had utilized this method to determine the applicability of UV disinfection in radiology and microbiological effects of pulsed xenon ultraviolet disinfection respectively (McGinn et al., 2021). Figure 2.12 illustrates the procedure to conduct the contact plate method.

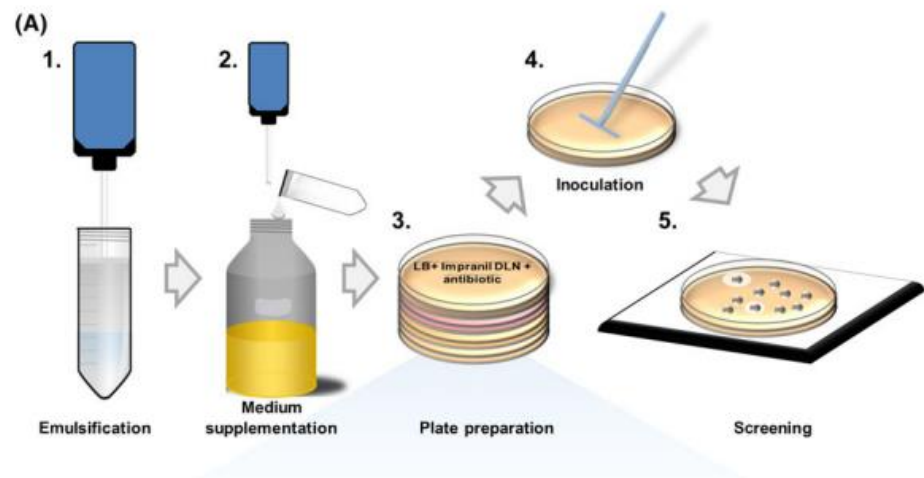


Figure 2.12: Procedure to Conduct Contact Plate Method

(Molitor et al., 2020)

2.5.2 Swab Method

Swab method is an approach to collect a sample by rolling it on a surface. In the standard procedure, it uses a sterile swab moistened with sterile saline to collect the sample and transfer it into a cultivation medium post-sampling. Although it is difficult to standardize and labor intensive, however it possesses a benefit of manipulation around uneven surfaces (Scott et al., 2022). In 2020, although Morikane et al. utilized the contact plate method to determine the microbiological effects in this study, he further applied swab method to compare the result between two different approaches (Morikane et al., 2020). In addition, Chen also utilized swab method in this study of evaluation of pulsed xenon ultraviolet light device (Chen et al., 2020). Figure 2.13 illustrates the recommended procedure to conduct the swab method.

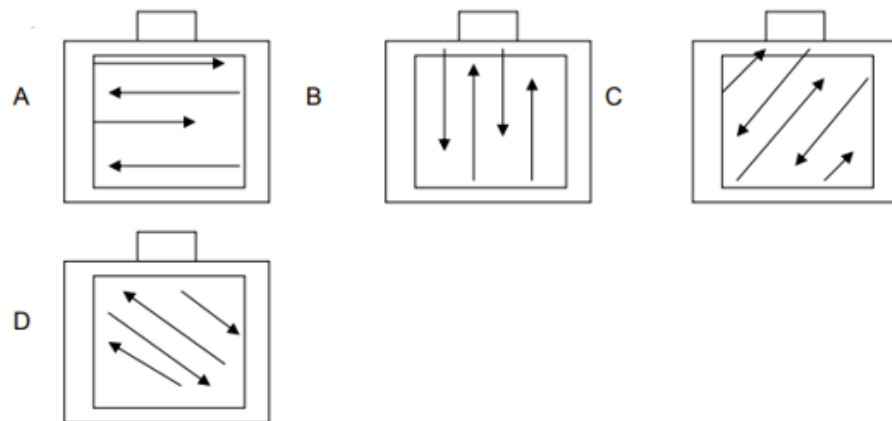


Figure 2.13: Recommended Procedure to Conduct Swab Method

(Public Health England, 2017)

2.5.3 Other Physical Sampling Method

Some of the other uncommon physical sampling method include sponges, sensitivity card and Formica sheet (Scott et al., 2022). The sponge method is known as using a sterile sponge that had been wiped across a sample and then placed in a bag with Phosphate-buffered saline (PBS) which will be processed in a lab blender. The processed fluid will be poured into the plates filled with agar and incubated before analysis (Thom et al., 2012); (Beal et al., 2016).

On the other hand, UV sensitivity card is another method to use for bioburden reduction. It is a device that record UV dose readings and is reliable in the determination of the position of UV device (Masse et al., 2018). However, it is not a suitable approach to identify the efficacy of UVGI and the efficacy will be very dependent on different factor such as material properties of substrate and type of microorganism (Gidari et al., 2021).

Formica sheet is another uncommon approach used to determine the efficacy of UVGI technology. It is a laminated composite material which is used on certain furniture. However, it is used by Rutala et al. to determine the efficacy in 2010. In his study, he inoculated certain quantity of vegetative bacteria on the Formica sheet and compared the data with contact plate sample after exposure to UVGI device (Rutala et al., 2010). Both approaches showed that the trend of reductions in colonies forming units (CFUs).

2.5.4 Computational Fluid Dynamics (CFD)

Computational Fluid Dynamics (CFD) had been also used to determine the performance of UVGI technology recently. CFD is an approach that utilizes numerical methods to perform engineering analysis that emphasizes on analyzing problems related to fluid characteristic. Therefore, it is commonly used in air disinfection to study the microorganism distribution in a specific environment related to COVID-19 pandemic such as airborne virus dispersion, modelling of sneezing and coughing, ventilation and facial mask design. For instance, Gilkeson & Noakes had conducted a study via CFD to predict the UVGI effectiveness in air disinfection (Gilkeson & Noakes, 2012). They had generated several plots of the dose in their paper using different types of turbulence model.

2.5.5 Optical Simulation Approach

Optical simulation approach is a valuable tool for analyzing spatial data and understand the potential impact of different scenarios. The software can be divided into 3 major categories, which named as sequential ray tracing, non-sequential ray tracing and finite-difference time-domain. Sequential ray tracing software utilizes algorithm that replaces the light source with directed rays, which use to consider optical effects such as chromatic aberration and reflection. It is ideal to use for lens system design (Klein, 2002). Next, non-sequential ray tracing software consider the coherence effects from reflection and absorption, which use to identify the behavior of different optical interaction between each object. It is suitable to use for

designing of complex optical system. Furthermore, the finite-difference time-domain software considers the electromagnetic wave propagation and is suitable to use for designing of micro-optical systems, which require a higher accuracy (Wiwanitkit, 2017). Optical simulation approach is commonly used in urban planning and transportation planning, however, is also used in environmental science and public health. For example, Hou et al. had performed a ray-tracing simulation to identify the effective disinfection coverage in upper zone of a room (Hou et al., 2021).

2.6 Log Reduction Value for Disinfection

In UVGI technology, Log Reduction Value (LRV) refers to the amount of reduction or inactivation of microorganisms such as bacteria, viruses, and other pathogens achieved by exposing them to a specific dose of UV-C radiation. It is a mathematical expression of the effectiveness of UVGI in reducing the number of microorganisms in certain area. It represents the degree to which the number of viable microorganisms has been reduced after a specified exposure time to UV-C radiation. It can be calculated by using equation (Tanner, 2015):

$$\text{Log Reduction} = \log_{10} \left(\frac{A}{B} \right)$$

Whereas,

A = Number of viable microorganism before treatment

B = Number of viable microorganism after treatment

For instance, a log reduction value of 1 indicates that 90% of the microorganisms have been eliminated, while a log reduction value of 2 represents a 99% reduction. Table 2.1 illustrates the percentage of reduction subject to level of log reduction.

Table 2.1: Percentage of Reduction subject to Log Reduction

Level of Log Reduction	Percentage of Reduction (%)
1	90
2	99
3	99.9
4	99.99
5	99.999
6	99.9999

A higher log reduction value means a more effective sterilization process. In practical terms, achieving a log reduction value of 3 or more is often considered necessary to ensure effective disinfection in healthcare settings or other high-risk environments (Derraik et al., 2020). Different types of microorganisms vary in their susceptibility to UV-C radiation. Some microorganisms are more resistant than others, and the log reduction value may vary accordingly. Table 2.2 indicates some examples of required dose needed to inactivate different pathogens. Table 2.3 also shows a table of required dose needed to inactivate SARS-Cov-2 for different level of LRV.

Table 2.2: Dose Required for Different Log Reduction Value

Type of Pathogens	Dose Required for 90% reduction ($mJ/(cm^2)$)	Dose Required for 99.9% reduction ($mJ/(cm^2)$)	Reference
Adenovirus type 2	40.0	119.0	Gerba et al. 2002
Calicivirus canine	7.0	22.0	Husman et al. 2004
Calicivirus feline	5.0	23.0	Thurston-Enriquez et al. 2003
Coxsackievirus B3	8.0	24.5	Gerba et al. 2002
Coxsackievirus B5	9.5	27.0	Gerba et al. 2002
Echovirus I	8.0	25.0	Gerba et al. 2002
Echovirus II	7.0	20.5	Gerba et al. 2002
Poliovirus 1	7.0	28.0	Thompson et al. 2003
Rotavirus	20.0	140.0	Caballero et al. 2004

Table 2.3: Dose Required for Disinfectant for SARS-Cov-2
(Sabino et al., 2020)

Viral inactivation for SARS-Cov-2 (%)	Dose Required for reduction ($mJ/(cm^2)$)
1 LRV (90%)	0.016
2 LRV (99%)	0.706
3 LRV (99.9%)	6.556
4 LRV (99.99%)	31.880
5 LRV (99.999%)	108.714

2.7 Summary

Based on the literature, distance from source to surface and intensity of source have crucial influence on the efficacy of UVGI performance. It is known that mercury lamps, pulsed lamps and UV emitting diodes are the major UVGI technology that commonly used in different industry such as HVAC industry, medical industry and agriculture industry. The common physical approach to collect the data include contact plate, swab, sponges, UV sensitivity card and Formica sheet. Virtual approach such as CFD and optical analysis give an early insight to the researcher to reduce excessive workload on physical trial and error. In this paper, the optical analysis will be selected to use as the approach for identifying the irradiation profile for surface disinfection. The efficacy of UVGI will be further determined based on the irradiation profile.

CHAPTER 3

METHODOLOGY

3.1 Project Process Flow

Figure 3.1 indicates a flowchart that map out the approach to complete this project. The flowchart illustrates the process from the beginning until the end of the project.

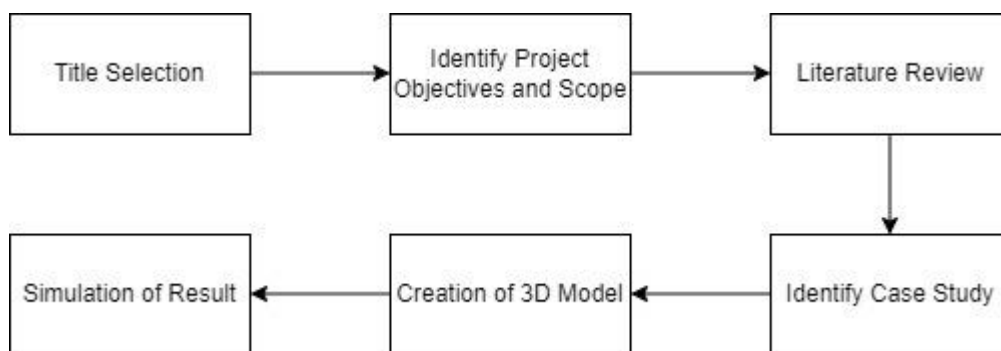


Figure 3.1: Project Flow Chart

Title selection is important as it predetermines the field of study of the project. Based on the selected title, objectives and scope can be identified to make sure the project is within capability and if there is any limitation. After title selection and setting objectives of this project, the progress moves on to researching on the UVGI technologies, factors that might impact the performance as well as the dose needed to inactivate pathogens. Literature review was done as well to obtain support information for the project. A comprehensive study on approach in identifying UVGI dose was also

reviewed to grasp a basic understanding of current methodology. Next, several 3D models with different configurations are created based on collected information and further analysis on the performance of UVGI technologies are also conducted using ANSYS SPEOS. The analysis is done to ensure the necessary dose needed to inactivate SARS-Cov-2 based on the literature review.

3.2 Gantt Chart

In order to ensure this project is completed in time, a project schedule is created using Gantt chart to act as a guide to ensure project is in progress as planned. The Gantt chart for this project schedule is separated into two parts as shown in Figure 3.2 and Figure 3.3.

Semester 1												
Activities (Week)	1	2	3	4	5	6	7	8	9	10	11	12
Literature Review Research	█	█	█	█	█	█	█	█	█	█	█	█
Report Writing			█	█	█	█	█	█	█	█	█	█
Learning on Simulation Tool (ANSYS SPEOS)								█	█	█	█	█
Identifying Methodology										█	█	█

Figure 3.2: Project Gantt Chart (1)

Semester 2												
Activities (Week)	1	2	3	4	5	6	7	8	9	10	11	12
Simulation on Case Study	█	█	█	█	█	█	█					
Analysis of Result												
Report Writing						█	█	█	█			
Finalize Report									█	█		
Presentation of Presentation Slide										█	█	
Project Presentation											█	█

Figure 3.3: Project Gantt Chart (2)

3.3 Identify Case Study

The study conducted in the research paper written by Wan Yunoh et al. in 2021 will be served as the basis for the case study. In their paper, the authors investigated the correlation between the irradiation profile at different distances and various types and power of light sources using physical prototype.

In this paper, a similar study will be conducted, however, the physical prototype approach will be replaced by optical simulation approach. In short, a model of UV Mobile Lamp with different intensity will be utilized as the UV light source, and a model of sensor will be created to act as the surface that received the irradiation from the light source. To ensure the setup is as close to the previous study, the models of the light source and sensor will possess a similar dimension to the equipment used in the previous paper.

After conducting several research, Philip TUV PL-L lamps series, which are commonly used in residential water and air disinfection unit were selected to use as the model of UV light source. The datasheet of Philip TUV PL-L lamps can be downloaded from the official website (Philips, 2022). The products with 36W and 55W will be selected as the parameter for the light source as they have the similar parameter as the one in reference paper. Figures 3.4 and 3.5 indicate the detail information regarding to the light source.

Product	D1 (max)	D (max)	A (max)	B (max)	C (max)
TUV PL-L 18W/4P 1CT/25	18 mm	39 mm	195 mm	220 mm	225 mm
TUV PL-L 36W/4P 1CT/25	18 mm	38 mm	385 mm	410 mm	415 mm
TUV PL-L 55W/4P HF 1CT/25	18 mm	38 mm	505 mm	530 mm	535 mm

Figure 3.4: Dimension of Bulb Label (Philips, 2022)

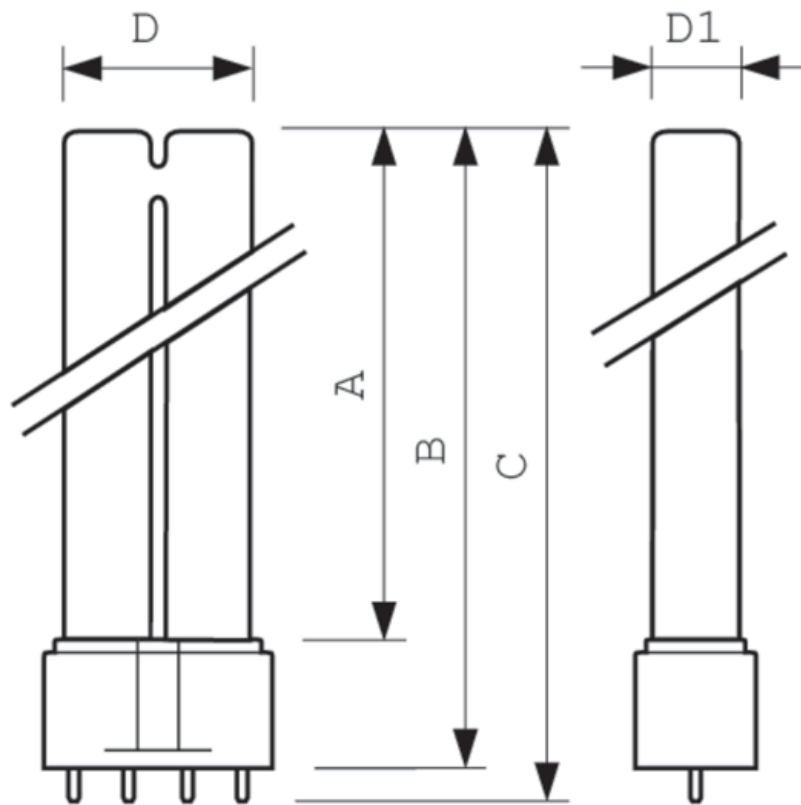


Figure 3.5: Illustration of the Light Bulb (Philips, 2022)

On the other hand, the dimension of ILT5000 will be selected to use as the model of UV sensor. The datasheet of ILT5000 can be downloaded from the official website as well. Noted that the dimension of the sensor suggests the area that used to measure and track the average irradiation profile. Figure 3.6 indicates the detail information regarding to the sensor.

DESCRIPTION	SPECIFICATIONS
<p>Effective Germicidal Detector</p> <p>Configured with a spectral response weighted to match the IES Luckiesh and DIN standards for germicidal effectiveness.</p> <p>Measurement Range: $3.00e^{-9}$ to $2.50e^{-3}$ effective Watts/cm²</p> <p>Germicidal Spectral Range: 235 – 307 nm, calibration wavelength at 270 nm</p> <p>Dimensions: 68 mm x 42 mm diameter</p> <p>Order part numbers: ILT5000*, SED240/ACT5/W (detector)</p> <p>* Software Included / Tablet PC Sold Separately</p>	

Figure 3.6: Specification of the Sensor

The SARS-CoV-2 pandemic has had a significant impact on the world since its emergence in late 2019, making it a primary target for scientists seeking to combat the virus. Therefore, this study will use SARS-CoV-2 as the pathogen sample for surface disinfection. Based on the literature review, log reduction values of 3, 4, and 5 are commonly used in the healthcare industry to ensure effective disinfection. As a result, the total dose required to disinfect SARS-CoV-2 has been defined as 6.556 mW/cm^2 , 31.880 mW/cm^2 and 108.714 mW/cm^2 .

3.4 Creation and Setup of Model

Two configurations of the models will be created to represent vertical setup and angled setup between sensor and the light source. The vertical setup is defined as the surface of the sensor is perpendicular to the light source while the angled setup is defined as the surface of the sensor is 45 degrees to the light source. The 3D model of the design will be generated using built in function in ANSYS SPEOS. Both dimension of the model is design according to the datasheet. Several configurations had been created to specify the distance between the light source with the sensor from 10 mm to 210 mm with an interval of 20 mm. Figure 3.7 and Figure 3.8 illustrates both of the 3D model configurations.

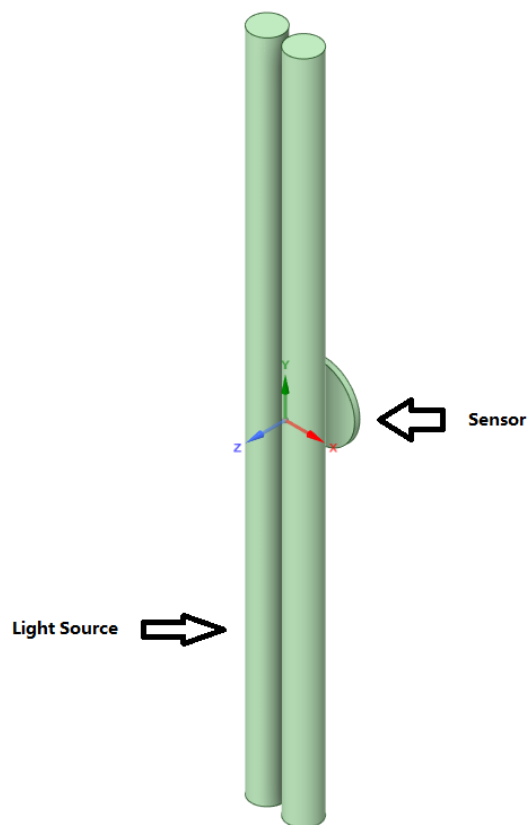


Figure 3.7: Sample of 3D Model for Vertical Setup

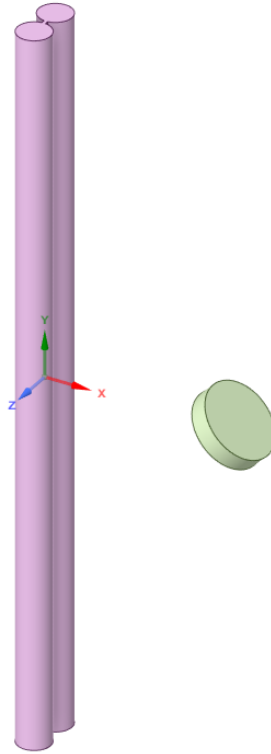


Figure 3.8: Sample of 3D Model for Angled Setup

Once the models were created, several optical simulations will be conducted with a monochromatic spectrum of 254nm. In the simulation setup, the light source is defined as Radiant flux with an intensity law that obey Lamberitian rule with an emission angle of 180 degree. The power of the light sources will be set to 36W and 55W according to the case study. On the other hand, the software irradiation tracking map will be located on the surface of sensor model, which help to track the magnitude of irradiance on surface area that defined by the sensor product matrix. Figures 3.9 and 3.10 illustrate the example of both the simulation settings. The irradiation profiles will be generated and tabulated in the end of simulation for the next step.

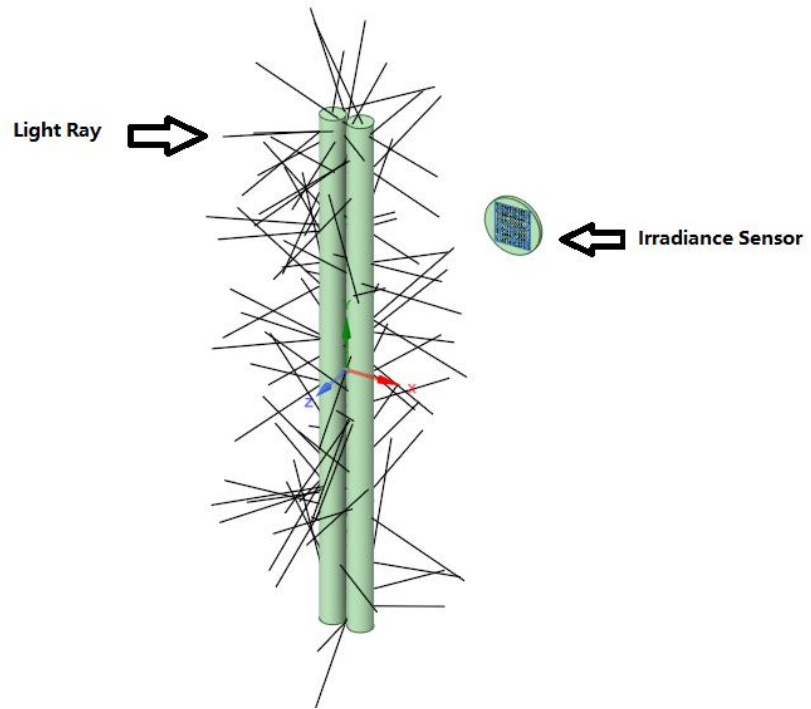


Figure 3.9: Sample Simulation Setting for Vertical Setup

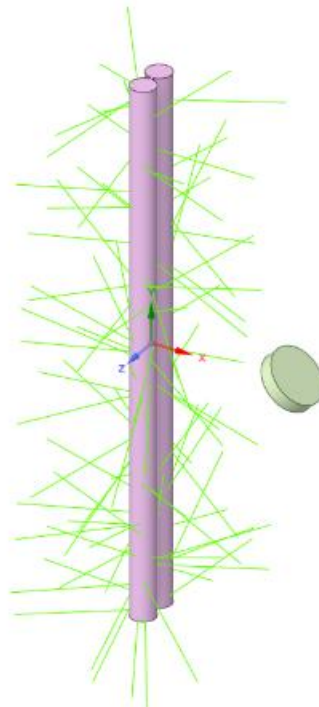


Figure 3.10: Sample Simulation Setting for Angled Setup

3.5 Identification of Exposure Time to Achieve Optimal Dose

In UVGI applications, the dose is an important parameter that determines the effectiveness of the disinfection process. The total dose can be resulted from low UVC power for a long duration, or high UVC power for a short duration. Generally, a higher dose of UV energy is required to kill or inactivate more resistant microorganisms, or to achieve a higher level of disinfection. In this project, SARS-Cov-2 will be selected as the sample to be disinfected, which subjected to LRV of 3, 4 and 5.

Based on the irradiation profile obtained from the previous step, the time required to reach the total dose in different distance will be calculated and tabulated. The required exposure time can be determined based on equation:

$$D = I * t$$

wherea,

$$D = Total\ Dose, \mu Ws/cm^2$$

$$I = UV\ Intensity, \mu W/cm^2$$

$$t = Exposure\ Time, s$$

CHAPTER 4

RESULTS AND DISCUSSION

4.1 ANSYS SPEOS Results for 36 W Light Source at Vertical Setup

The analysis was done on the spatial behavior of 36 W light source to determine the irradiation profile with various distance from 10 mm to 210 mm with an interval of 20 mm. The results obtained had been shown in Figures 4.1 to 4.11.

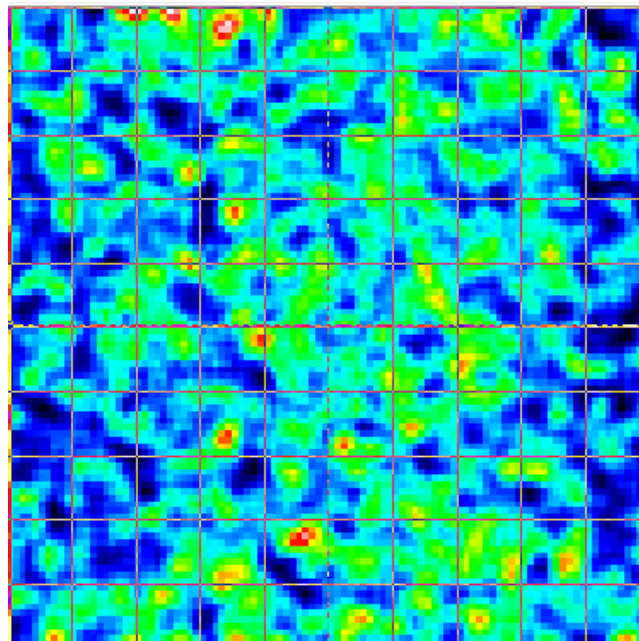


Figure 4.1: Irradiation Profile at 10 mm

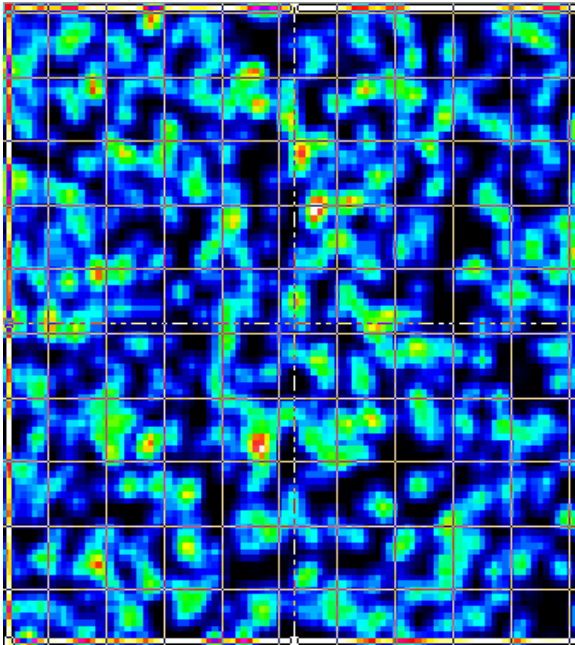


Figure 4.2: Irradiation Profile at 30 mm

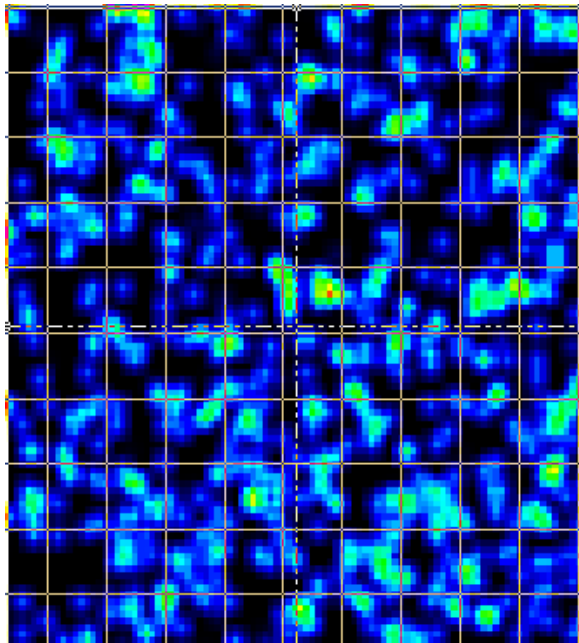


Figure 4.3: Irradiation Profile at 50 mm

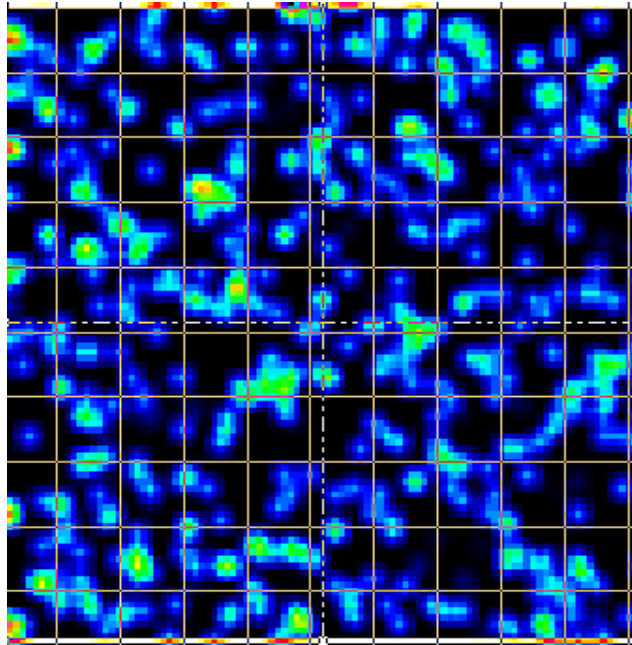


Figure 4.4: Irradiation Profile at 70 mm

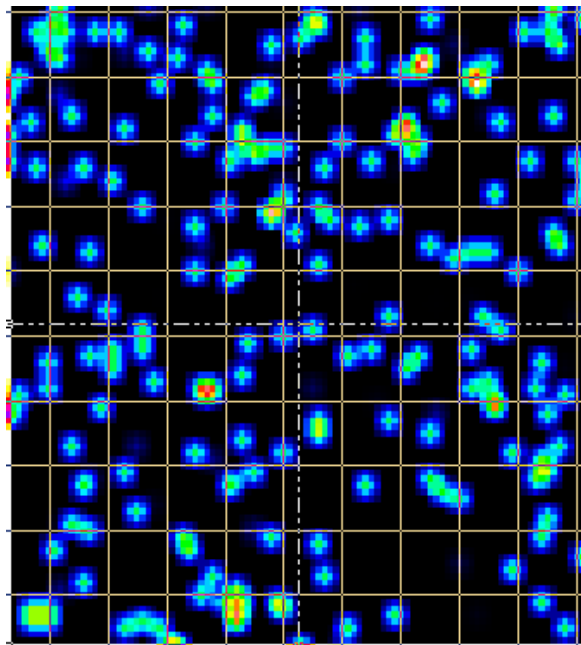


Figure 4.5: Irradiation Profile at 90 mm

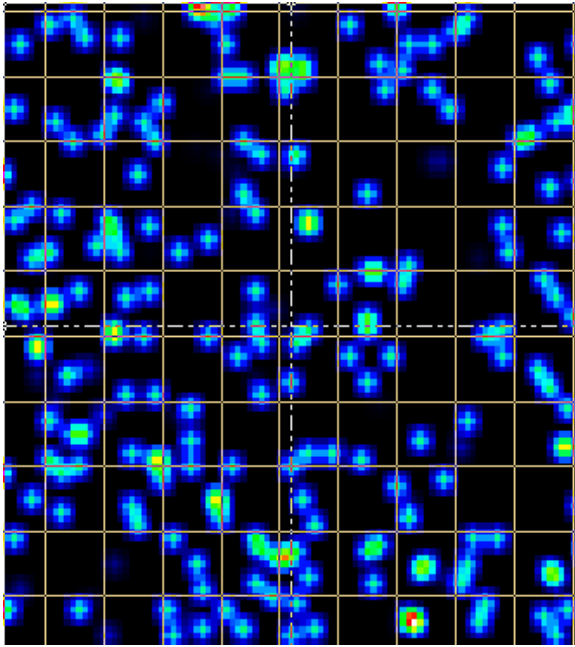


Figure 4.6: Irradiation Profile at 110 mm

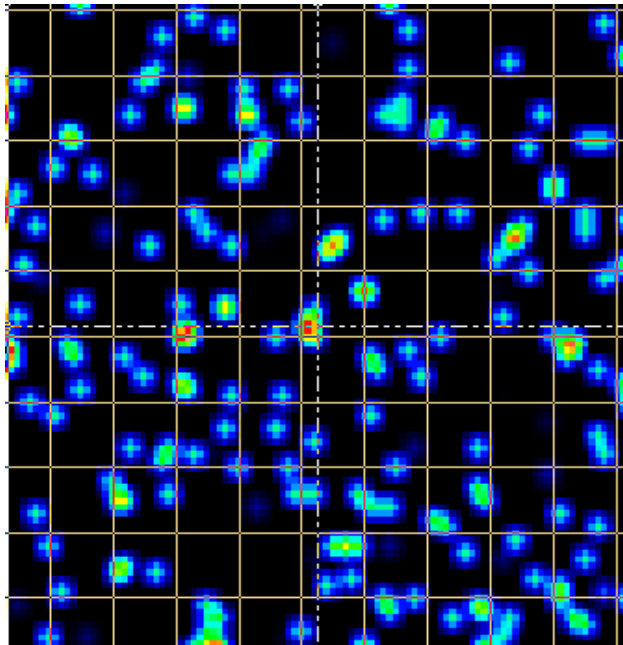


Figure 4.7: Irradiation Profile at 130 mm

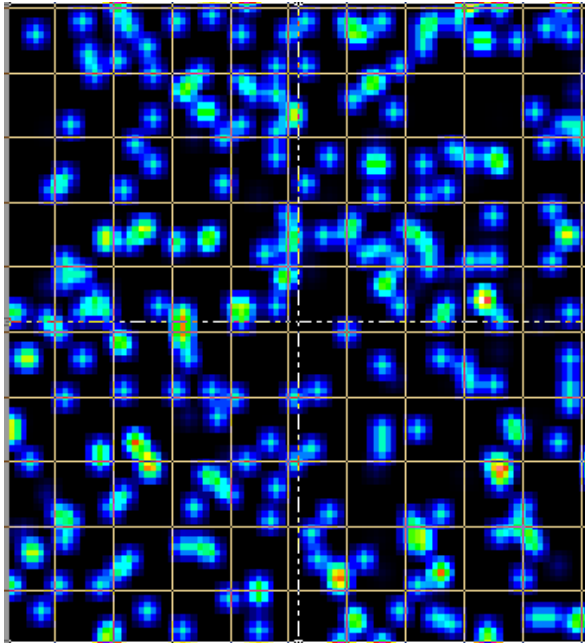


Figure 4.8: Irradiation Profile at 150 mm

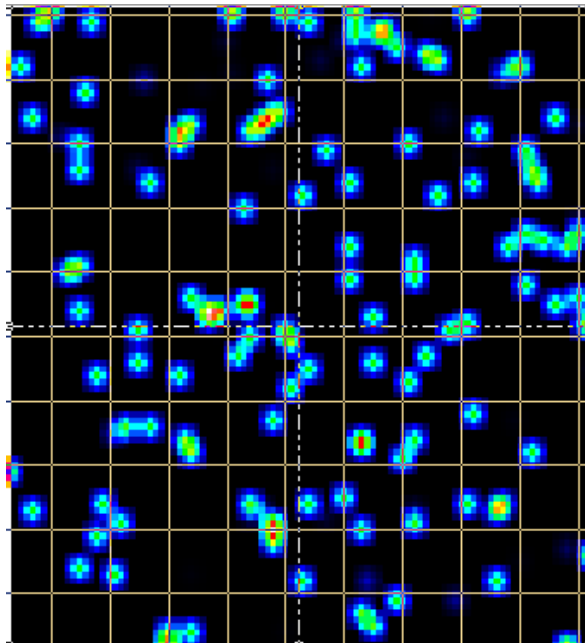


Figure 4.9: Irradiation Profile at 170 mm

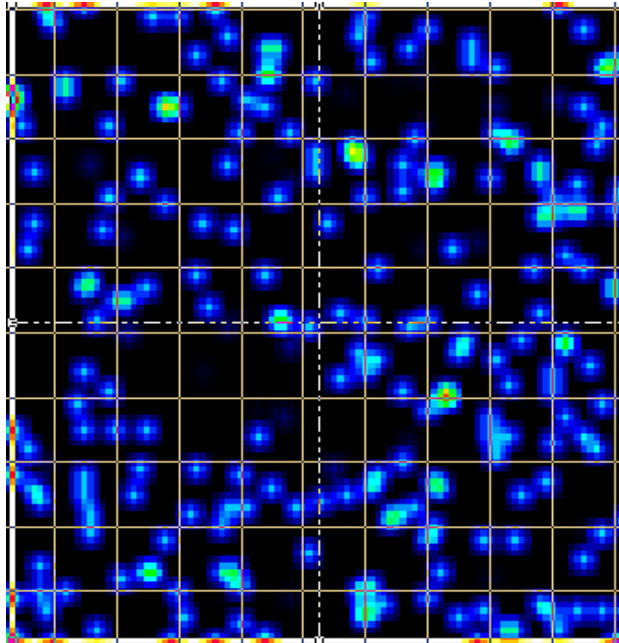


Figure 4.10: Irradiation Profile at 190 mm

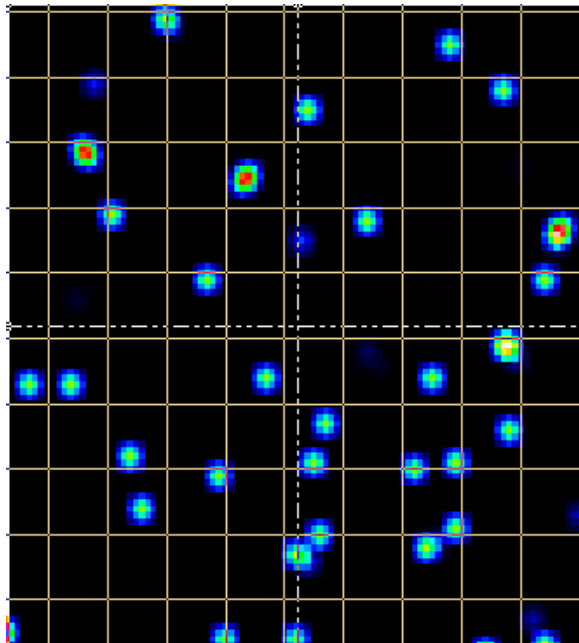


Figure 4.11: Irradiation Profile at 210 mm

Based on the irradiation profile, the average irradiation obtained by the sensor can be probed using built in tools. The average irradiation received by the sensor had been shown in Figures 4.12 to 4.22.

Magnitude	Operator	Measure	Thresholds	Value
irradiance	None	Average		0.00654945 W/cm ²

Figure 4.12: Average irradiation obtained by sensor at 10 mm

Magnitude	Operator	Measure	Thresholds	Value
irradiance	None	Average		0.0039172 W/cm ²

Figure 4.13: Average irradiation obtained by sensor at 30 mm

Magnitude	Operator	Measure	Thresholds	Value
irradiance	None	Average		0.00276351 W/cm ²

Figure 4.14: Average irradiation obtained by sensor at 50 mm

Magnitude	Operator	Measure	Thresholds	Value
irradiance	None	Average		0.00162343 W/cm ²

Figure 4.15: Average irradiation obtained by sensor at 70 mm

Magnitude	Operator	Measure	Thresholds	Value
irradiance	None	Average		0.000945149 W/cm ²

Figure 4.16: Average irradiation obtained by sensor at 90 mm

Magnitude	Operator	Measure	Thresholds	Value
irradiance	None	Average		0.000848014 W/cm ²

Figure 4.17: Average irradiation obtained by sensor at 110 mm

Magnitude	Operator	Measure	Thresholds	Value
irradiance	None	Average		0.000810587 W/cm ²

Figure 4.18: Average irradiation obtained by sensor at 130 mm

Magnitude	Operator	Measure	Thresholds	Value
irradiance	None	Average		0.000744227 W/cm ²

Figure 4.19: Average irradiation obtained by sensor at 150 mm

Magnitude	Operator	Measure	Thresholds	Value
irradiance	None	Average		0.000514727 W/cm ²

Figure 4.20: Average irradiation obtained by sensor at 170 mm

Magnitude	Operator	Measure	Thresholds	Value
irradiance	None	Average		0.000164006 W/cm ²

Figure 4.21: Average irradiation obtained by sensor at 190 mm

Magnitude	Operator	Measure	Thresholds	Value
irradiance	None	Average		0.00107482 W/cm ²

Figure 4.22: Average irradiation obtained by sensor at 210 mm

4.2 ANSYS SPEOS Results for 55 W Light Source at Vertical Setup

The analysis was done on the spatial behavior of 55 W light source to determine the irradiation profile with various distance from 10 mm to 210 mm with an interval of 20 mm. The results obtained had been shown in Figures 4.23 to 4.33.

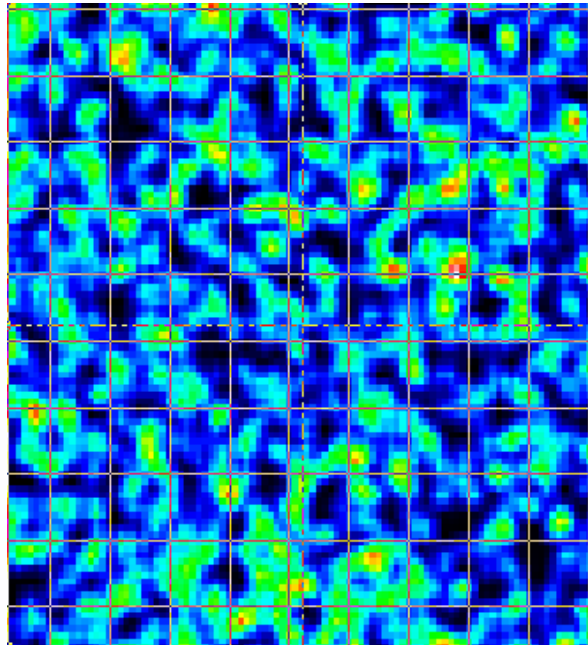


Figure 4.23: Irradiation Profile at 10 mm

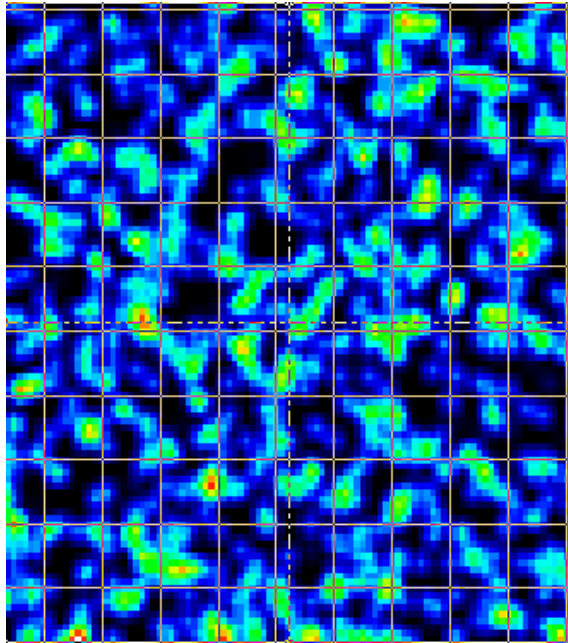


Figure 4.24: Irradiation Profile at 30 mm

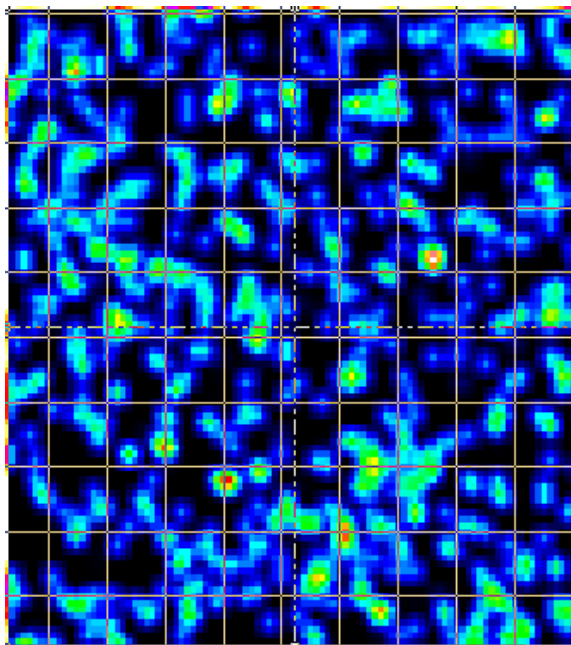


Figure 4.25: Irradiation Profile at 50 mm

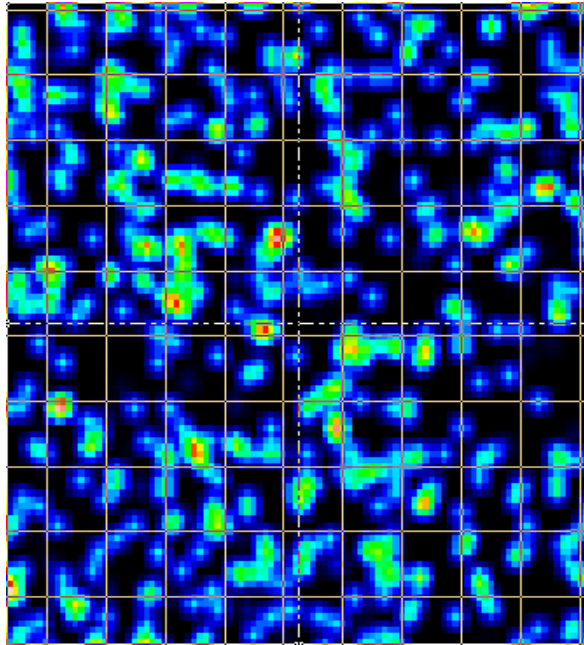


Figure 4.26: Irradiation Profile at 70 mm

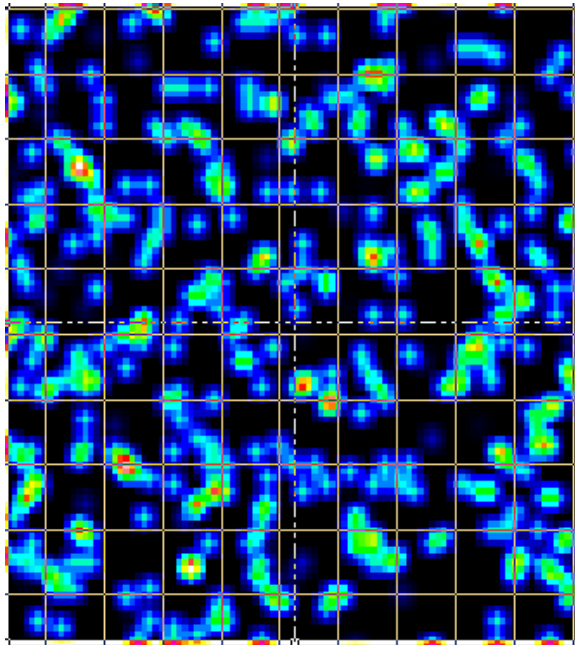


Figure 4.27: Irradiation Profile at 90 mm

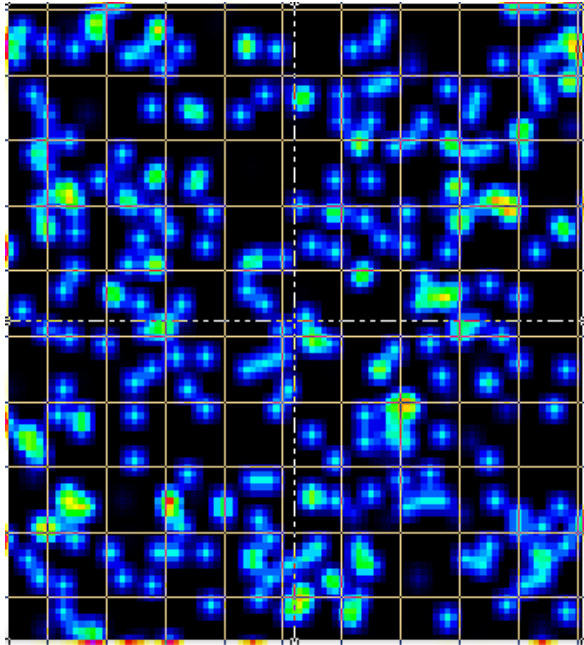


Figure 4.28: Irradiation Profile at 110 mm

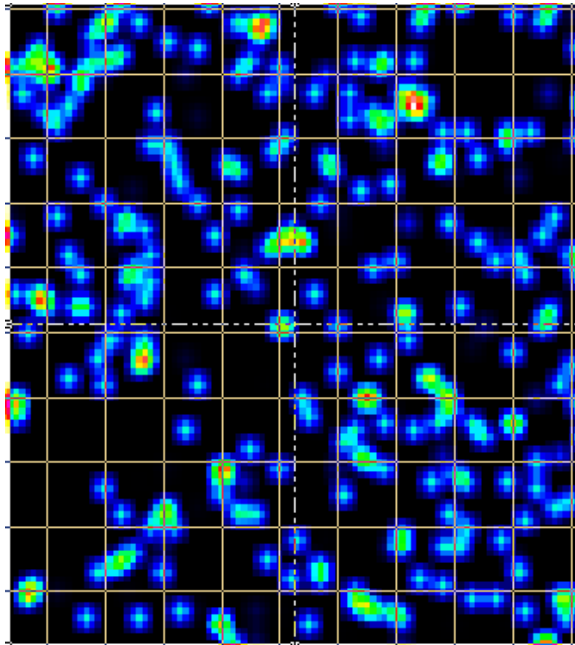


Figure 4.29: Irradiation Profile at 130 mm

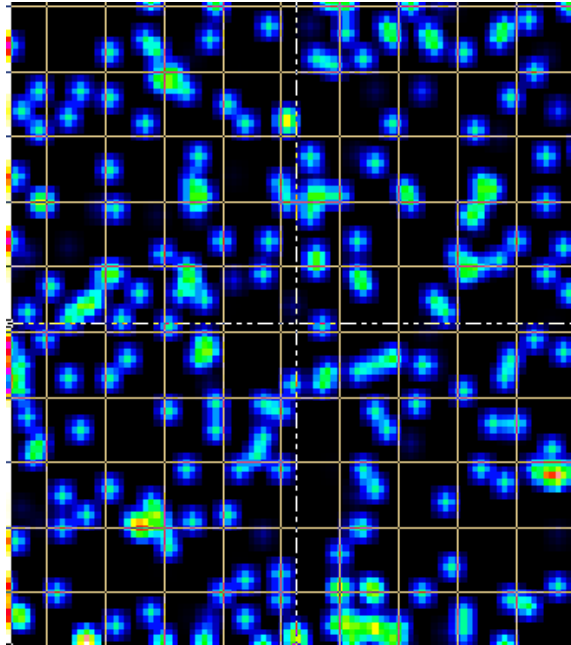


Figure 4.30: Irradiation Profile at 150 mm

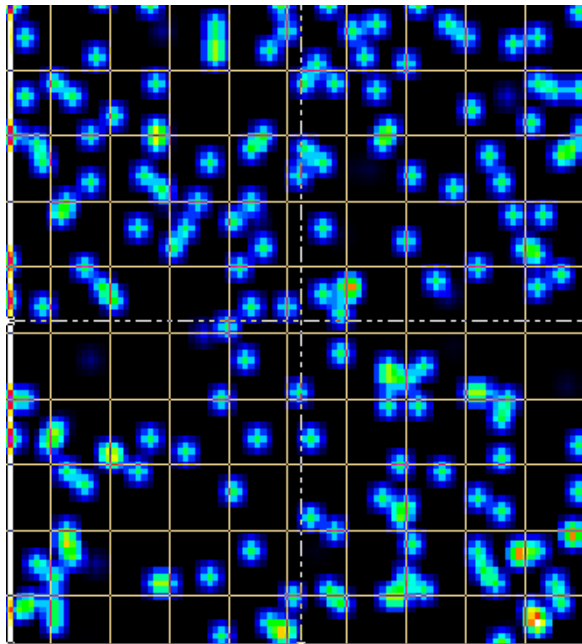


Figure 4.31: Irradiation Profile at 170 mm

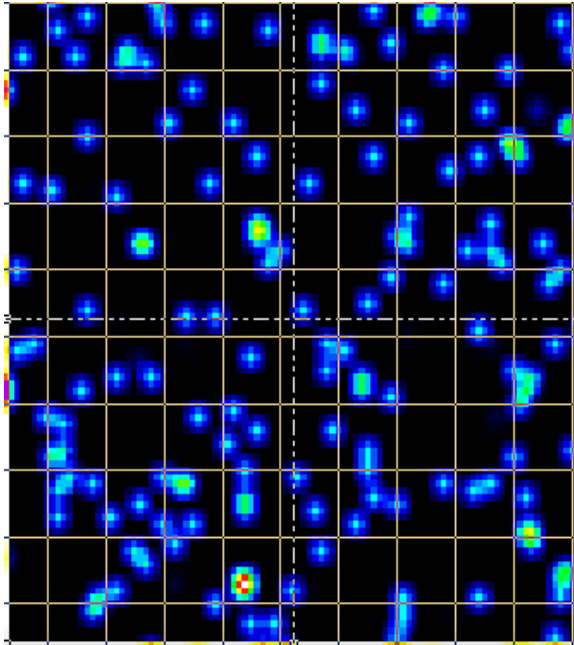


Figure 4.32: Irradiation Profile at 190 mm

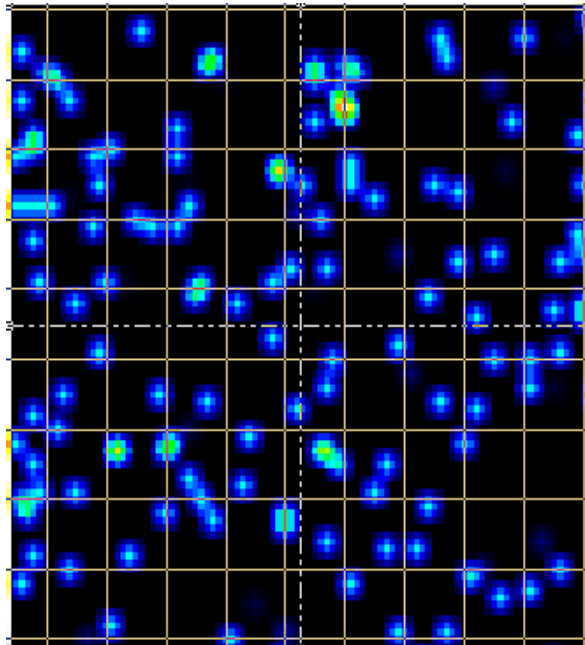


Figure 4.33: Irradiation Profile at 210 mm

Based on the irradiation profile, the average irradiation obtained by the sensor can be probed using built in tools. The average irradiation received by the sensor had been shown in Figures 4.34 to 4.44.

Magnitude	Operator	Measure	Thresholds	Value
irradiance	None	Average		0.0119192 W/cm ²

Figure 4.34: Average irradiation obtained by sensor at 10 mm

Magnitude	Operator	Measure	Thresholds	Value
irradiance	None	Average		0.00683092 W/cm ²

Figure 4.35: Average irradiation obtained by sensor at 30 mm

Magnitude	Operator	Measure	Thresholds	Value
irradiance	None	Average		0.00480308 W/cm ²

Figure 4.36: Average irradiation obtained by sensor at 50 mm

Magnitude	Operator	Measure	Thresholds	Value
irradiance	None	Average		0.00288473 W/c...

Figure 4.37: Average irradiation obtained by sensor at 70 mm

Magnitude	Operator	Measure	Thresholds	Value
irradiance	None	Average		0.00216111 W/cm ²

Figure 4.38: Average irradiation obtained by sensor at 90 mm

Magnitude	Operator	Measure	Thresholds	Value
irradiance	None	Average		0.00175227 W/cm ²

Figure 4.39: Average irradiation obtained by sensor at 110 mm

Magnitude	Operator	Measure	Thresholds	Value
irradiance	None	Average		0.0015284 W/cm ²

Figure 4.40: Average irradiation obtained by sensor at 130 mm

Magnitude	Operator	Measure	Thresholds	Value
irradiance	None	Average		0.00131021 W/cm ²

Figure 4.41: Average irradiation obtained by sensor at 150 mm

Magnitude	Operator	Measure	Thresholds	Value
irradiance	None	Average		0.0009007 W/cm ²

Figure 4.42: Average irradiation obtained by sensor at 170 mm

Magnitude	Operator	Measure	Thresholds	Value
irradiance	None	Average		0.000812402 W/cm ²

Figure 4.43: Average irradiation obtained by sensor at 190 mm

Magnitude	Operator	Measure	Thresholds	Value
irradiance	None	Average		0.000720558 W/cm ²

Figure 4.44: Average irradiation obtained by sensor at 210 mm

4.3 ANSYS SPEOS Results for 36 W Light Source at Angled Setup

The analysis was done on the spatial behavior of 36 W light source to determine the irradiation profile with various distance from 10 mm to 210 mm with an interval of 20 mm. The results obtained had been shown in Figures 4.45 to 4.55.

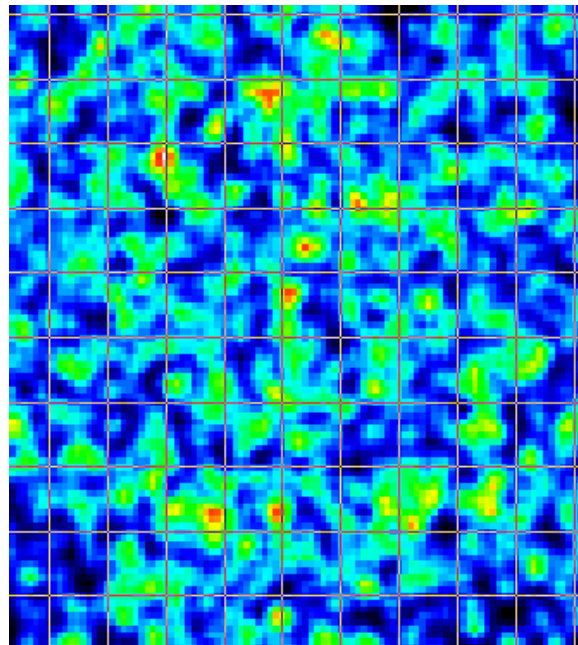


Figure 4.45: Irradiation Profile at 10 mm

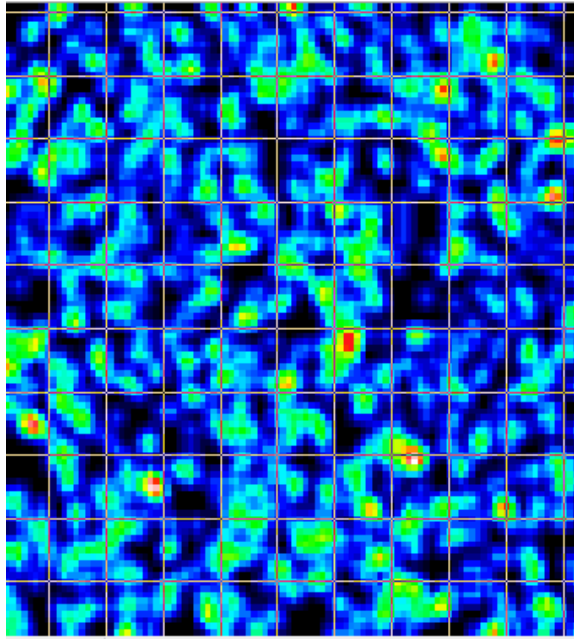


Figure 4.46: Irradiation Profile at 30 mm

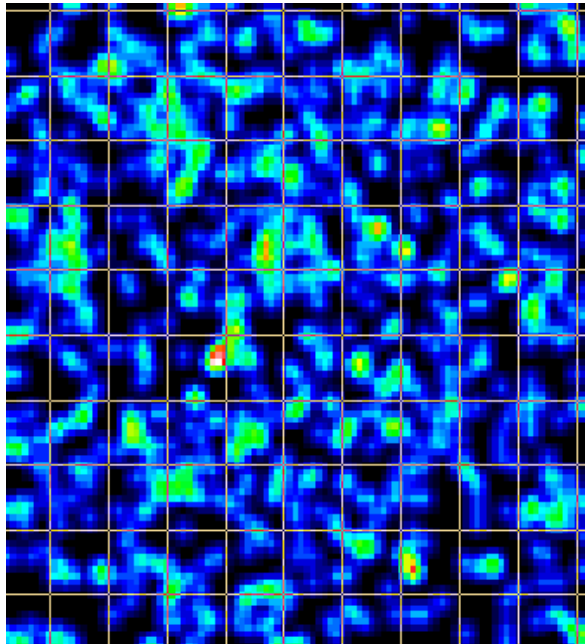


Figure 4.47: Irradiation Profile at 50 mm

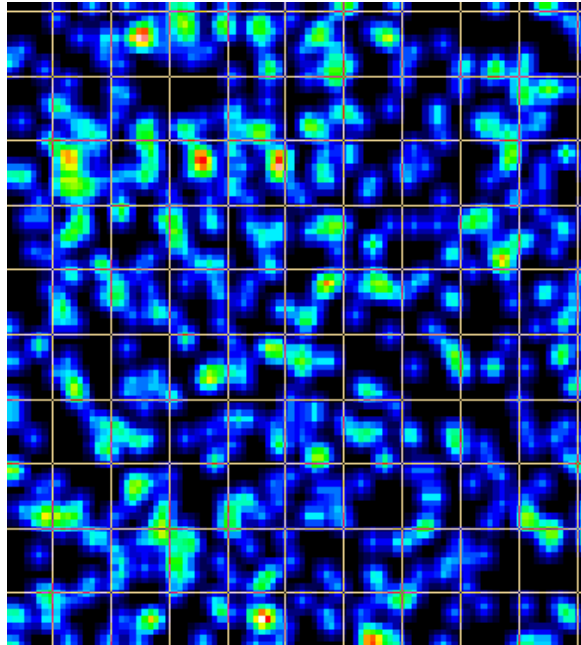


Figure 4.48: Irradiation Profile at 70 mm

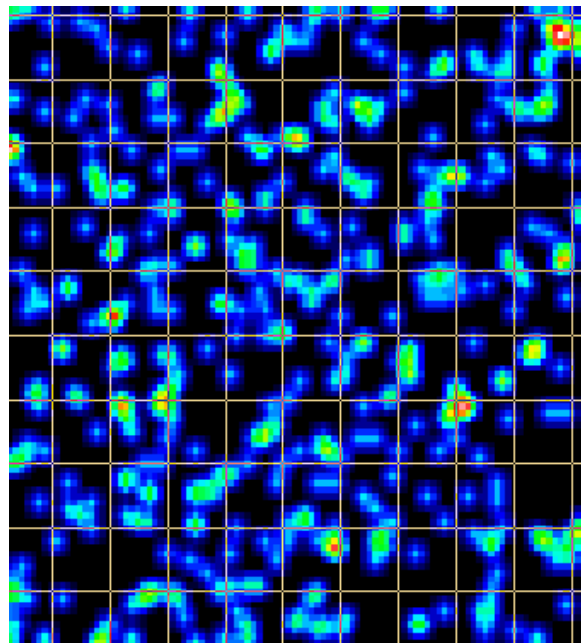


Figure 4.49: Irradiation Profile at 90 mm

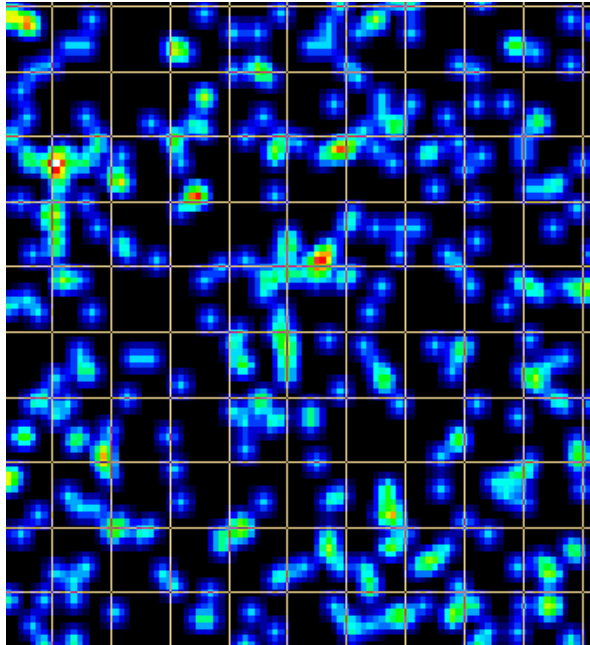


Figure 4.50: Irradiation Profile at 110 mm

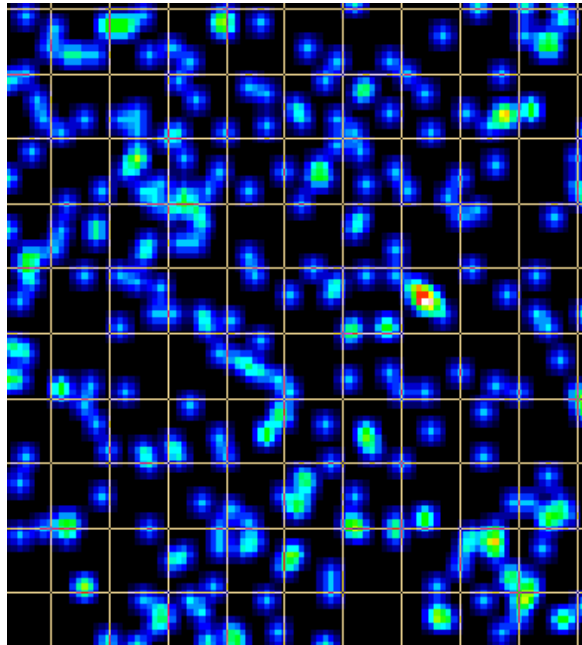


Figure 4.51: Irradiation Profile at 130 mm

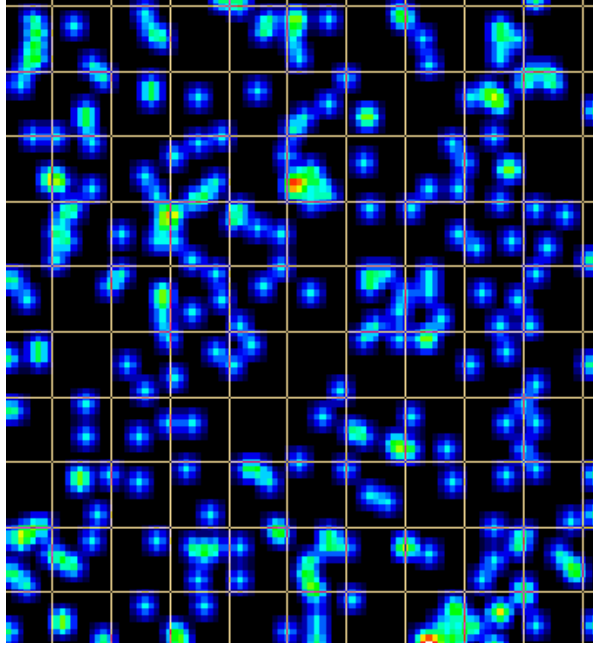


Figure 4.52: Irradiation Profile at 150 mm

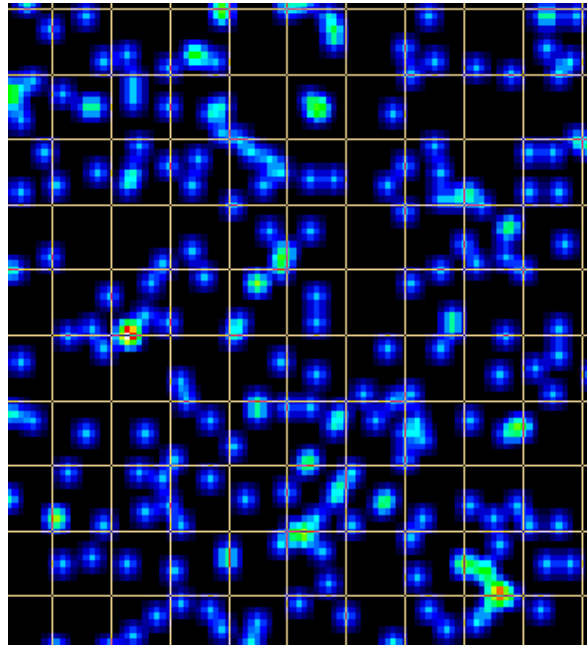


Figure 4.53: Irradiation Profile at 170 mm

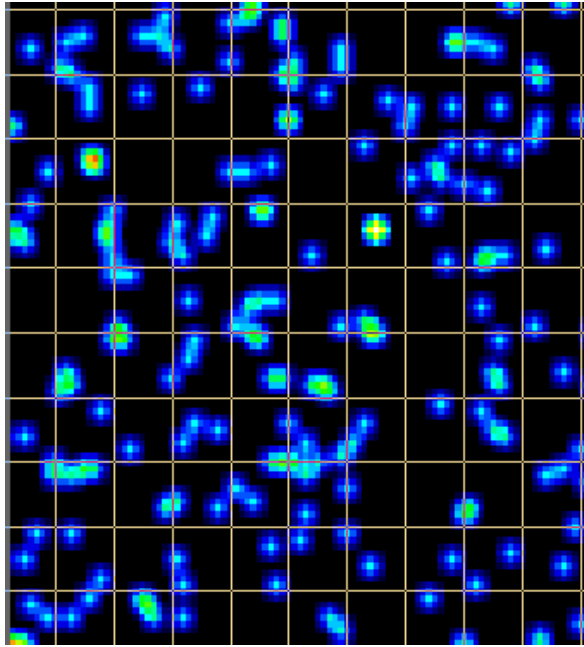


Figure 4.54: Irradiation Profile at 190 mm

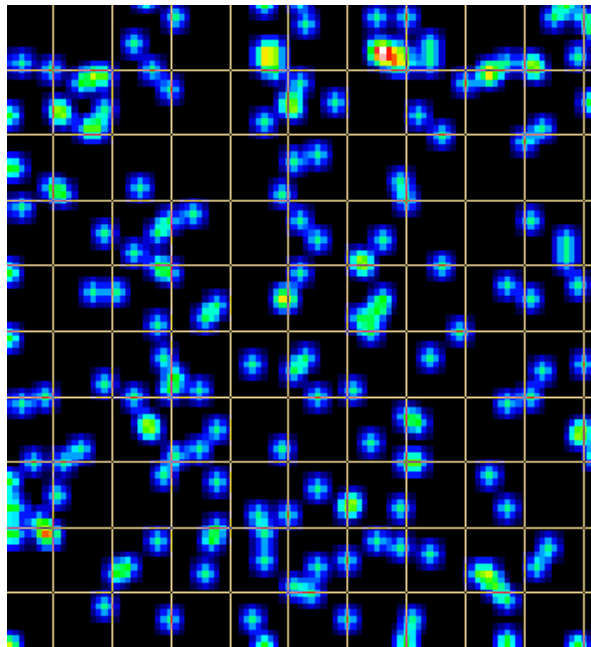


Figure 4.55: Irradiation Profile at 210 mm

Based on the irradiation profile, the average irradiation obtained by the sensor can be probed using built in tools. The average irradiation received by the sensor had been shown in Figures 4.56 to 4.66.

Magnitude	Operator	Measure	Thresholds	Value
irradiance	None	Average		0.00468518 W/cm ²

Figure 4.56: Average irradiation obtained by sensor at 10 mm

Magnitude	Operator	Measure	Thresholds	Value
irradiance	None	Average		0.00302262 W/cm ²

Figure 4.57: Average irradiation obtained by sensor at 30 mm

Magnitude	Operator	Measure	Thresholds	Value
irradiance	None	Average		0.00226279 W/cm ²

Figure 4.58: Average irradiation obtained by sensor at 50 mm

Magnitude	Operator	Measure	Thresholds	Value
irradiance	None	Average		0.00152425 W/cm ²

Figure 4.59: Average irradiation obtained by sensor at 70 mm

Magnitude	Operator	Measure	Thresholds	Value
irradiance	None	Average		0.000773863 W/cm ²

Figure 4.60: Average irradiation obtained by sensor at 90 mm

Magnitude	Operator	Measure	Thresholds	Value
irradiance	None	Average		0.000489225 W/cm ²

Figure 4.61: Average irradiation obtained by sensor at 110 mm

Magnitude	Operator	Measure	Thresholds	Value
irradiance	None	Average		0.000384373 W/cm ²

Figure 4.62: Average irradiation obtained by sensor at 130 mm

Magnitude	Operator	Measure	Thresholds	Value
irradiance	None	Average		0.000346493 W/cm ²

Figure 4.63: Average irradiation obtained by sensor at 150 mm

Magnitude	Operator	Measure	Thresholds	Value
irradiance	None	Average		0.000294253 W/cm ²

Figure 4.64: Average irradiation obtained by sensor at 170 mm

Magnitude	Operator	Measure	Thresholds	Value
irradiance	None	Average		3.41665e-05 W/cm ²

Figure 4.65: Average irradiation obtained by sensor at 190 mm

Magnitude	Operator	Measure	Thresholds	Value
irradiance	None	Average		3.01639e-05 W/cm ²

Figure 4.66: Average irradiation obtained by sensor at 210 mm

4.4 ANSYS SPEOS Results for 55 W Light Source at Angled Setup

The analysis was done on the spatial behavior of 36 W light source to determine the irradiation profile with various distance from 10 mm to 210 mm with an interval of 20 mm. The results obtained had been shown in Figures 4.67 to 4.77.

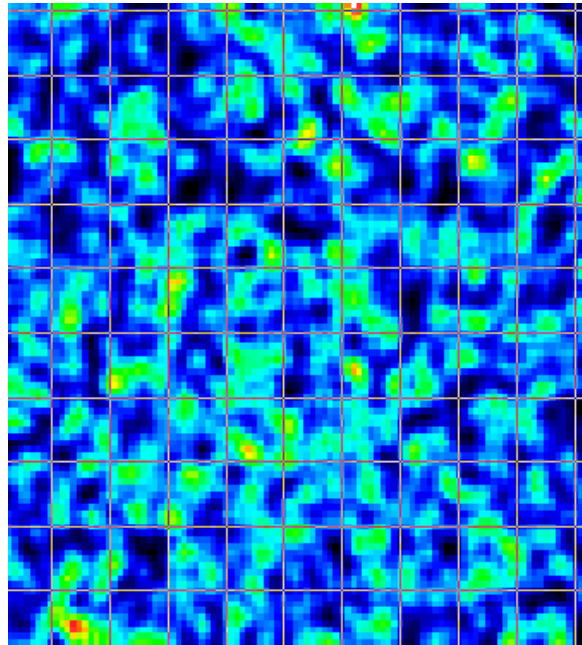


Figure 4.67: Irradiation Profile at 10 mm

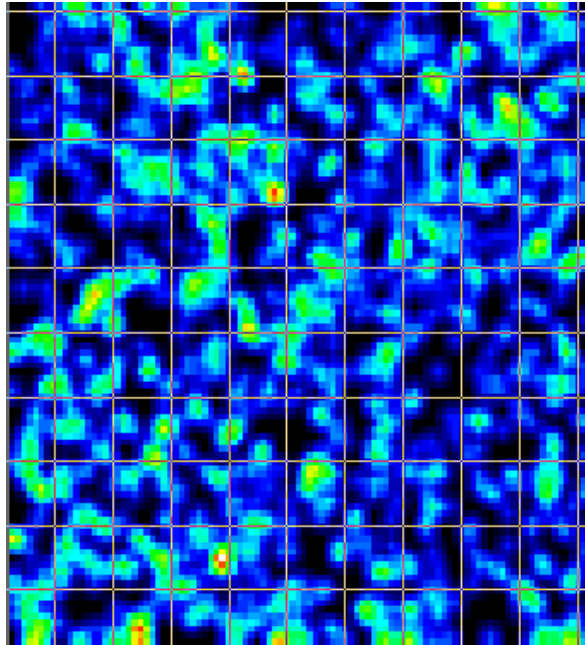


Figure 4.68: Irradiation Profile at 30 mm

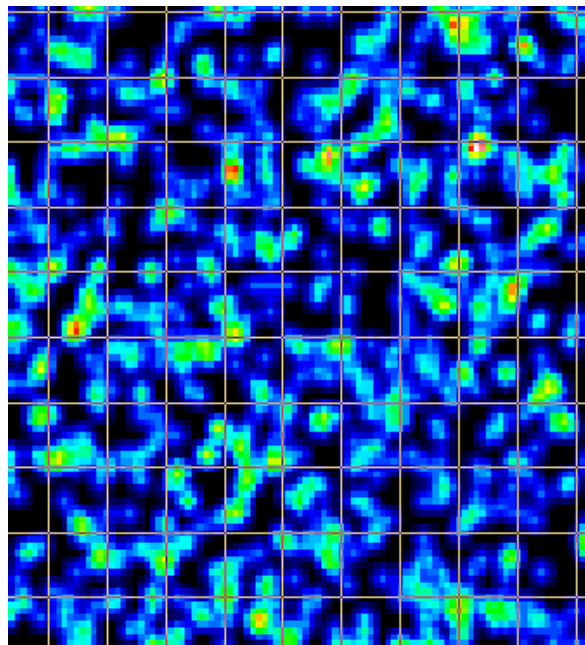


Figure 4.69: Irradiation Profile at 50 mm

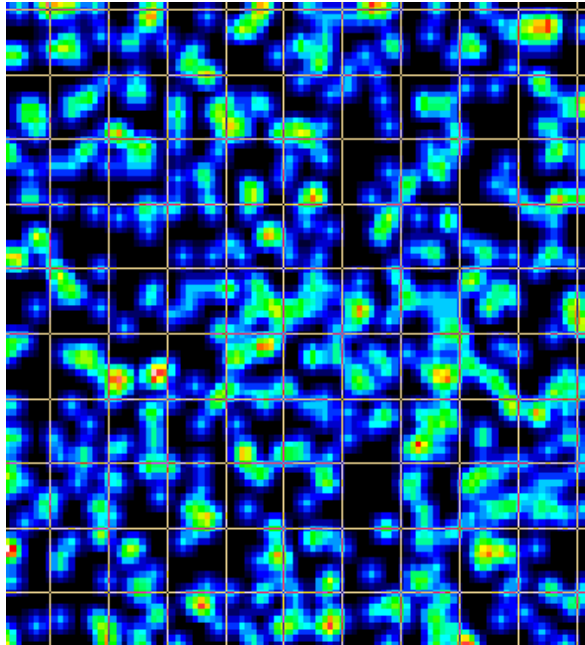


Figure 4.70: Irradiation Profile at 70 mm

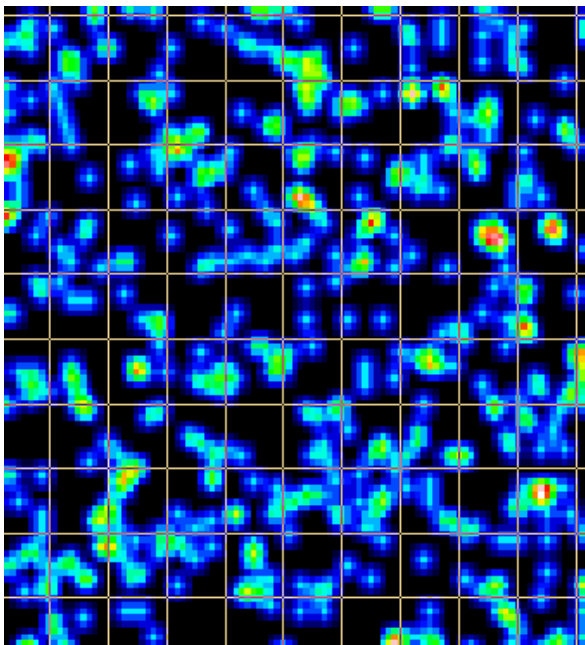


Figure 4.71: Irradiation Profile at 90 mm

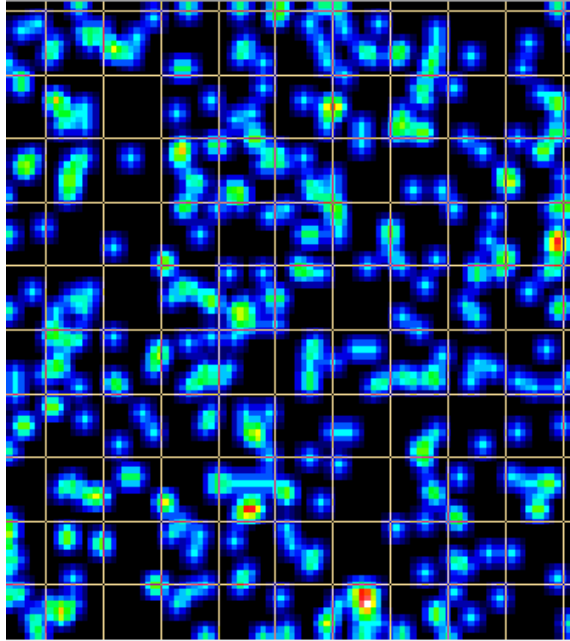


Figure 4.72: Irradiation Profile at 110 mm

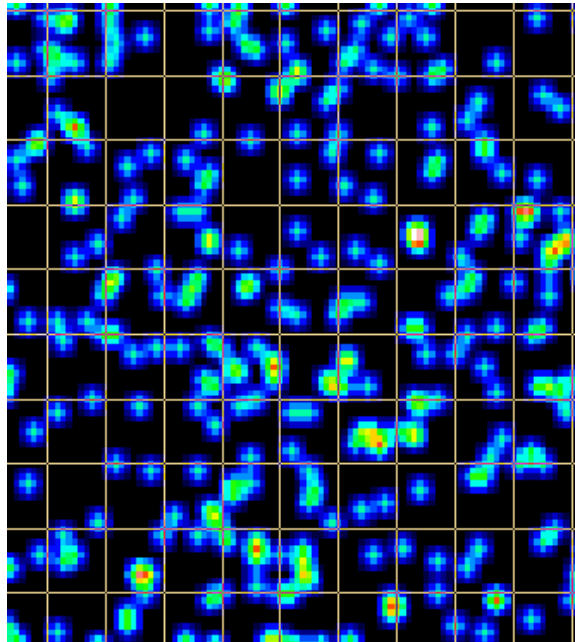


Figure 4.73: Irradiation Profile at 130 mm

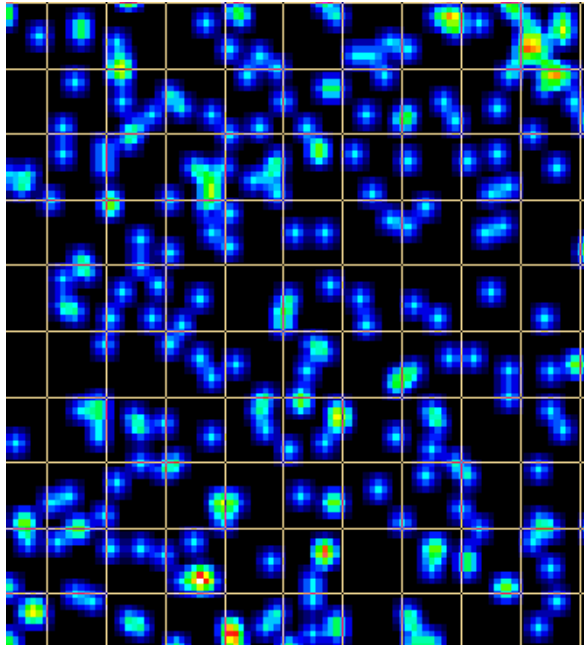


Figure 4.74: Irradiation Profile at 150 mm

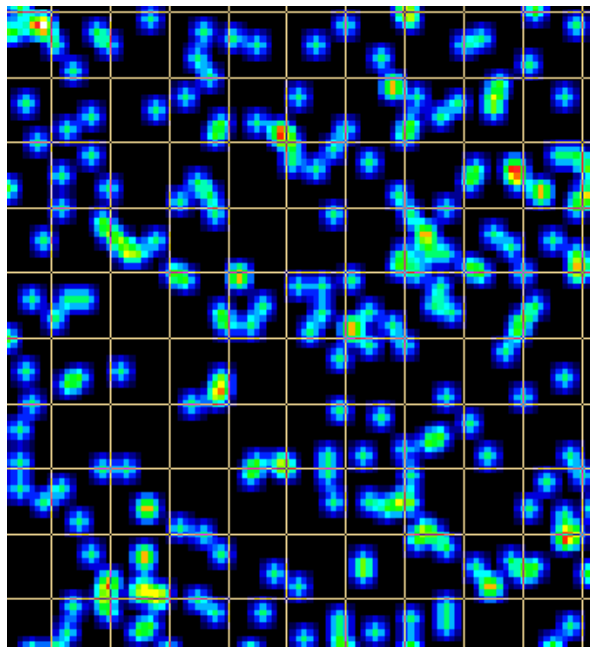


Figure 4.75: Irradiation Profile at 170 mm

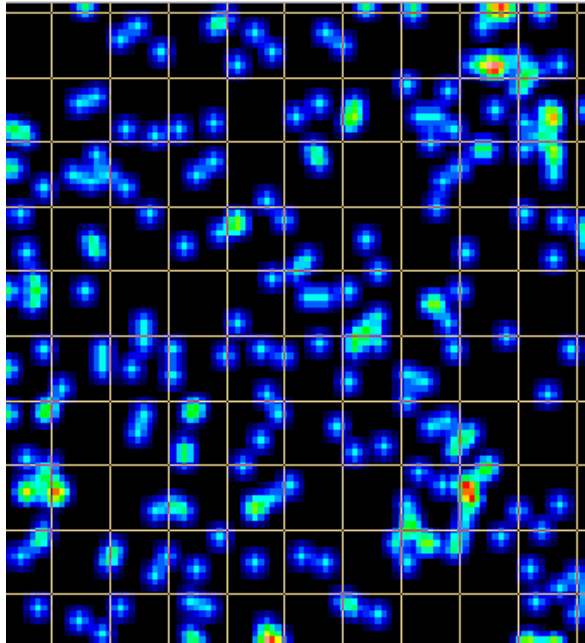


Figure 4.76: Irradiation Profile at 190 mm

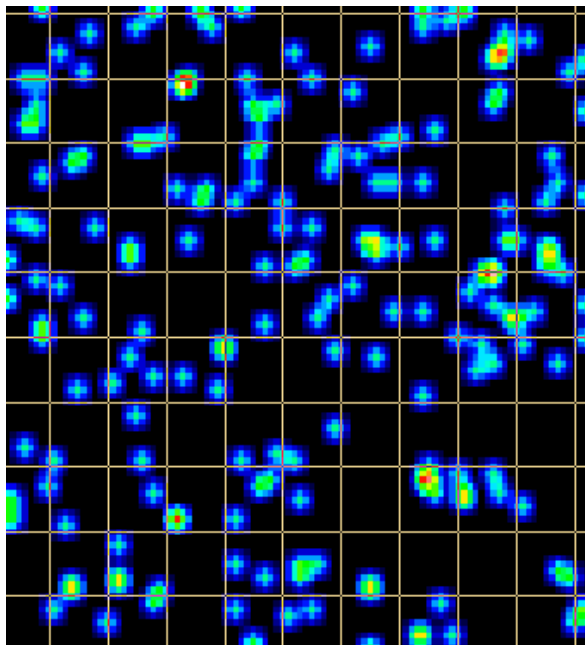


Figure 4.77: Irradiation Profile at 210 mm

Based on the irradiation profile, the average irradiation obtained by the sensor can be probed using built in tools. The average irradiation received by the sensor had been shown in Figures 4.78 to 4.88.

Magnitude	Operator	Measure	Thresholds	Value
irradiance	None	Average		0.0102221 W/cm ²

Figure 4.78: Average irradiation obtained by sensor at 10 mm

Magnitude	Operator	Measure	Thresholds	Value
irradiance	None	Average		0.00449178 W/cm ²

Figure 4.79: Average irradiation obtained by sensor at 30 mm

Magnitude	Operator	Measure	Thresholds	Value
irradiance	None	Average		0.00311454 W/cm ²

Figure 4.80: Average irradiation obtained by sensor at 50 mm

Magnitude	Operator	Measure	Thresholds	Value
irradiance	None	Average		0.002203 W/cm ²

Figure 4.81: Average irradiation obtained by sensor at 70 mm

Magnitude	Operator	Measure	Thresholds	Value
irradiance	None	Average		0.00142955 W/cm ²

Figure 4.82: Average irradiation obtained by sensor at 90 mm

Magnitude	Operator	Measure	Thresholds	Value
irradiance	None	Average		0.001229 W/cm ²

Figure 4.83: Average irradiation obtained by sensor at 110 mm

Magnitude	Operator	Measure	Thresholds	Value
irradiance	None	Average		0.00102912 W/cm ²

Figure 4.84: Average irradiation obtained by sensor at 130 mm

Magnitude	Operator	Measure	Thresholds	Value
irradiance	None	Average		0.00084822 W/cm ²

Figure 4.85: Average irradiation obtained by sensor at 150 mm

Magnitude	Operator	Measure	Thresholds	Value
irradiance	None	Average		0.000756119 W/cm ²

Figure 4.86: Average irradiation obtained by sensor at 170 mm

Magnitude	Operator	Measure	Thresholds	Value
irradiance	None	Average		0.000678873 W/cm ²

Figure 4.87: Average irradiation obtained by sensor at 190 mm

Magnitude	Operator	Measure	Thresholds	Value
irradiance	None	Average		0.000583306 W/cm ²

Figure 4.88: Average irradiation obtained by sensor at 210 mm

4.5 Post-Process of Result

The results obtained from section 4.1, 4.2, 4.3 and 4.4 were further tabulated and several graphs were generated to identify the relation between different power of light source and the average irradiation detected by the sensor at different position for both configurations.

Table 4.1 and Figure 4.89 indicate the tabulated data and graph for the vertical setup from ANSYS SPEOS. Noted that the unit of the irradiance was converted from mW/cm² into μ W/cm².

Table 4.1: Average Irradiation versus Distance at different Power Source for Vertical Setup

Distance From Light Source (mm)	Average Irradiation Detected by Sensor (μ W/cm ²)										
	10	30	50	70	90	110	130	150	170	190	210
Power Source = 36W	6549.450	3917.200	2763.510	1623.430	945.150	848.010	810.590	744.230	514.730	164.010	107.480
Power Source = 55W	11919.200	6830.920	4803.080	2884.730	2161.110	1752.270	1528.400	1310.210	900.700	812.400	720.560

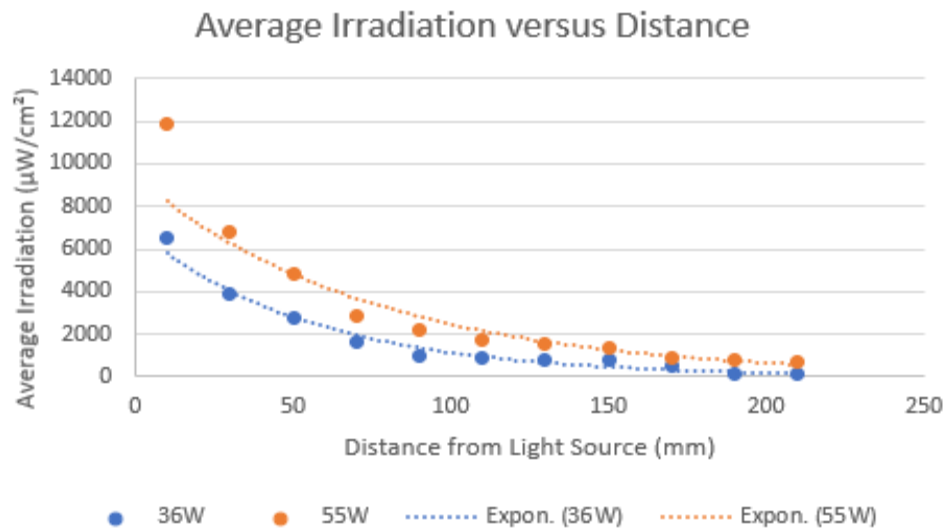


Figure 4.89: Average Irradiation versus Distance at different Power Source for Vertical Setup

Table 4.2 and Figure 4.90 indicate the tabulated data and graph for the angled setup from ANSYS SPEOS. Noted that the unit of the irradiance was also converted from mW/cm² into μ W/cm².

Table 4.2: Average Irradiation versus Distance at different Power Source for Angled Setup

Distance From Light Source (mm)	Average Irradiation Detected by Sensor (μ W/cm ²)										
	10	30	50	70	90	110	130	150	170	190	210
Power Source = 36W	4685.180	3022.620	2262.790	1524.250	773.863	489.225	384.373	346.493	294.253	34.167	30.164
Power Source = 55W	10222.100	4491.780	3114.540	2203.000	1429.550	1229.000	1029.120	848.220	756.119	678.873	583.306

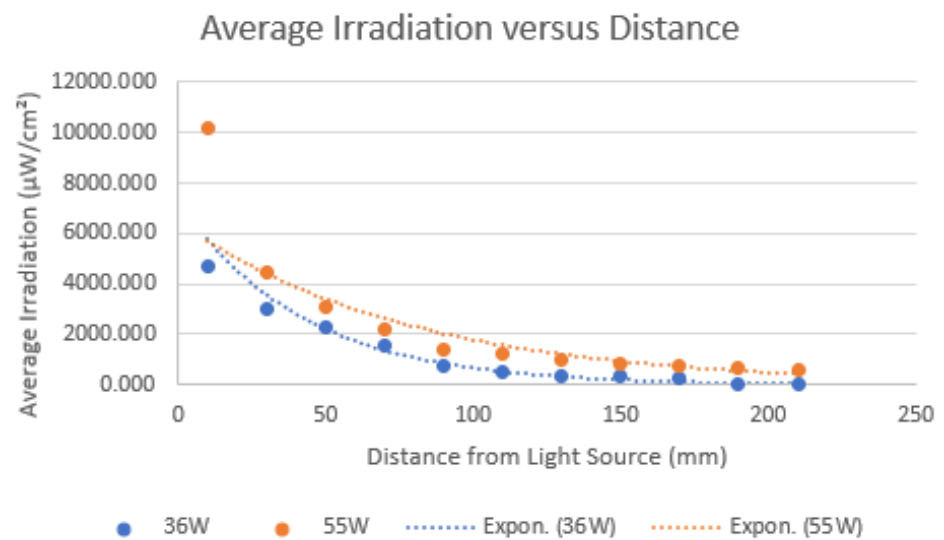


Figure 4.90: Average Irradiation versus Distance at different Power Source for Angled Setup

Based on the results, it can be concluded that the average irradiation detected by the sensor decreased as the distance from the light source increased. This observation was consistent for both the 36 W and 55 W light source in both configurations. It was also observed that the overall average irradiation detected was lower for the 36 W light source compared to the 55 W light source. Furthermore, the difference in irradiation gap between the two light sources was higher for the range between 10 mm to 70 mm compared to the range between 90 mm to 210 mm. This suggests that the distance range between 10 mm to 70 mm is more critical for effective UV-C disinfection, and the power of the light source is a significant factor in this range. In addition, the overall average irradiance of vertical configuration is higher than the angled configuration, this mean that the sensor possesses a better performance when it is face perpendicularly to the light source.

Based on the case study, the total dose to inactive SARS-Cov-2 at a LRV of 3, 4 and 5 will be 6.556 mW/cm^2 , 31.880 mW/cm^2 and 108.714 mW/cm^2 , which is equivalent to $6556 \text{ }\mu\text{W/cm}^2$, $31880 \text{ }\mu\text{W/cm}^2$ and $108714 \text{ }\mu\text{W/cm}^2$. The total exposure time needed for the sample at different distance and to reach the total dose can be calculated based on the equation:

$$D = I * t$$

$$t = \frac{D}{I}$$

wherea,

$$D = \text{Required Dose in } \mu\text{Ws/cm}^2$$

$$I = \text{Average Irradiation Detected by Sensor in } \mu\text{W/cm}^2$$

$$t = \text{Exposure Time, s}$$

For example, in vertical configuration, the average irradiation detected by sensor at 130 mm for 36 W power source are 810.590 $\mu\text{W}/\text{cm}^2$. The expected exposure time at LRV of 3 for this case can be calculated by:

$$t = \frac{D}{I}$$

$$t = \frac{6556 \mu\text{Ws}/\text{cm}^2}{810.59 \mu\text{W}/\text{cm}^2}$$

$$t = 8.088\text{s}$$

Table 4.3 to 4.5 indicate the tabulated data for total exposure time required to reach LRV of 3, 4 and 5 respectively at vertical configuration.

Table 4.3: Total Required Exposure Time Required to Reach 3 LRV for Vertical Configuration

Distance From Light Source (mm)	Exposure Time to reach 6556 $\mu\text{W}/\text{cm}^2$ (s)										
	10	30	50	70	90	110	130	150	170	190	210
Power Source = 36W	1.001	1.674	2.372	4.038	6.936	7.731	8.088	8.809	12.737	39.973	60.997
Power Source = 55W	0.550	0.960	1.365	2.273	3.034	3.741	4.289	5.004	7.279	8.070	9.098

Table 4.4: Total Required Exposure Time Required to Reach 4 LRV for Vertical Configuration

Distance From Light Source (mm)	Exposure Time to reach 31880 $\mu\text{W}/\text{cm}^2$ (s)										
	10	30	50	70	90	110	130	150	170	190	210
Power Source = 36W	4.868	8.138	11.536	19.637	33.730	37.594	39.329	42.836	61.935	194.378	296.613
Power Source = 55W	2.675	4.667	6.637	11.051	14.752	18.194	20.858	24.332	35.395	39.242	44.243

Table 4.5: Total Required Exposure Time Required to Reach 5 LRV for Vertical Configuration

Distance From Light Source (mm)	Exposure Time to reach 108714 $\mu\text{W}/\text{cm}^2$ (s)										
	10	30	50	70	90	110	130	150	170	190	210
Power Source = 36W	16.599	27.753	39.339	66.966	115.023	128.199	134.117	146.076	211.206	662.850	1011.481
Power Source = 55W	9.121	15.915	22.634	37.686	50.305	62.042	71.129	82.974	120.699	133.818	150.874

Figure 4.91 to 4.93 indicate the graph for total exposure time required to reach LRV of 3, 4 and 5 respectively at vertical configuration.

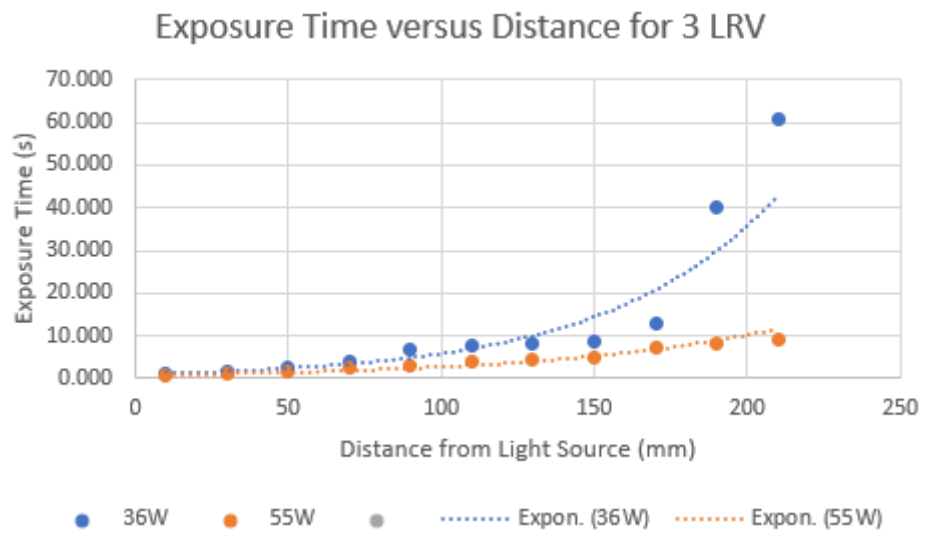


Figure 4.91: Total Required Exposure Time Required to Reach 3 LRV for Vertical Configuration

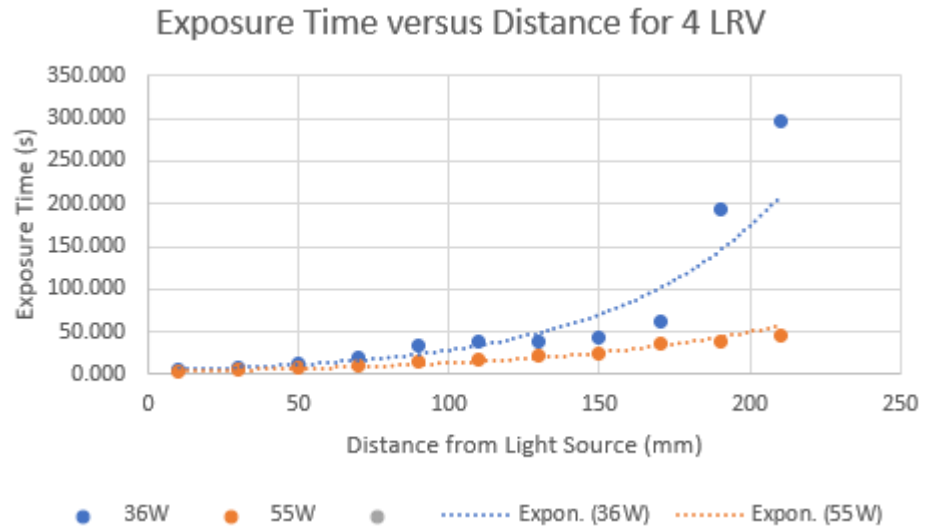


Figure 4.92: Total Required Exposure Time Required to Reach 4 LRV for Vertical Configuration

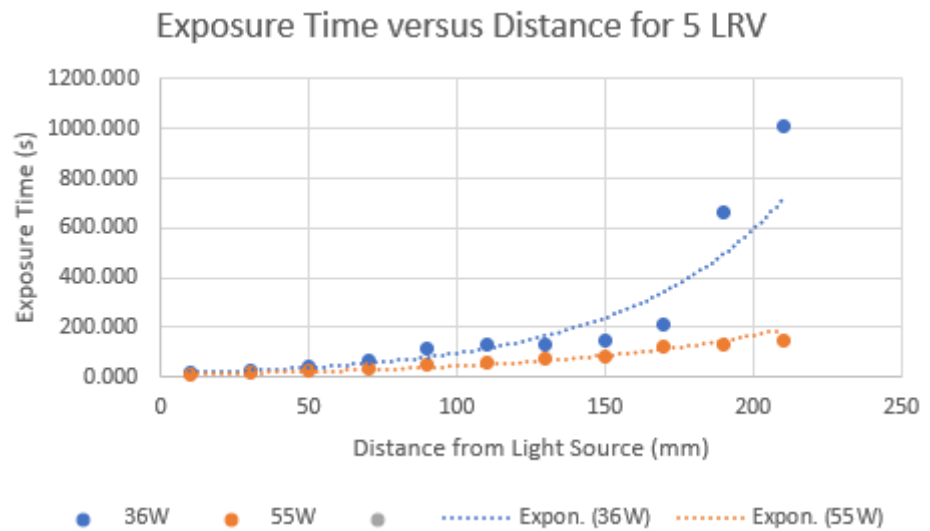


Figure 4.93: Total Required Exposure Time Required to Reach 5 LRV for Vertical Configuration

Table 4.6 to 4.8 indicate the tabulated data for total exposure time required to reach LRV of 3, 4 and 5 respectively at angled configuration.

Table 4.6: Total Required Exposure Time Required to Reach 3 LRV for Angled Configuration

Distance From Light Source (mm)	Exposure Time to reach 6556.000 $\mu\text{W}/\text{cm}^2$ (s)										
	10	30	50	70	90	110	130	150	170	190	210
Power Source = 36W	1.399	2.169	2.897	4.301	8.472	13.401	17.056	18.921	22.280	191.881	217.345
Power Source = 55W	0.641	1.460	2.105	2.976	4.586	5.334	6.370	7.729	8.671	9.657	11.239

Table 4.7: Total Required Exposure Time Required to Reach 4 LRV for Angled Configuration

Distance From Light Source (mm)	Exposure Time to reach 31880.000 $\mu\text{W}/\text{cm}^2$ (s)										
	10	30	50	70	90	110	130	150	170	190	210
Power Source = 36W	6.804	10.547	14.089	20.915	41.196	65.164	82.940	92.008	108.342	933.064	1056.889
Power Source = 55W	3.119	7.097	10.236	14.471	22.301	25.940	30.978	37.585	42.163	46.960	54.654

Table 4.8: Total Required Exposure Time Required to Reach 5 LRV for Angled Configuration

Distance From Light Source (mm)	Exposure Time to reach 108714.000 $\mu\text{W}/\text{cm}^2$ (s)										
	10	30	50	70	90	110	130	150	170	190	210
Power Source = 36W	23.204	35.967	48.044	71.323	140.482	222.217	282.835	313.755	369.458	3181.842	3604.098
Power Source = 55W	10.635	24.203	34.905	49.348	76.048	88.457	105.638	128.167	143.779	160.139	186.376

Figure 4.94 to 4.96 indicate the graph for total exposure time required to reach LRV of 3, 4 and 5 respectively at angled configuration.

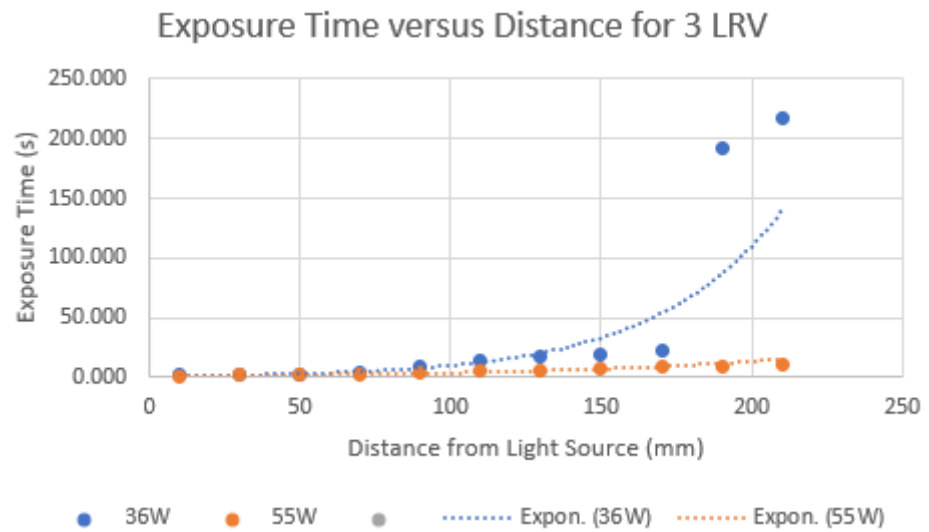


Figure 4.94: Total Required Exposure Time Required to Reach 3 LRV for Angled Configuration

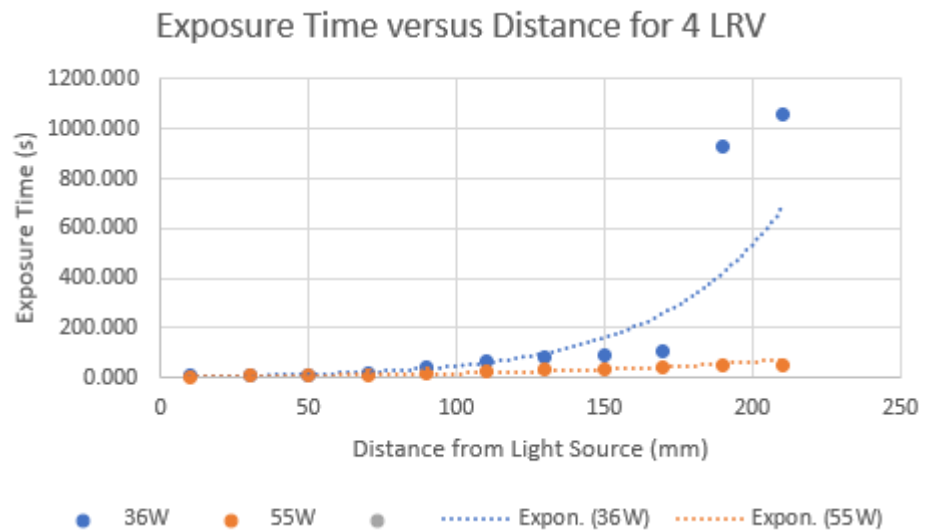


Figure 4.95: Total Required Exposure Time Required to Reach 4 LRV for Angled Configuration

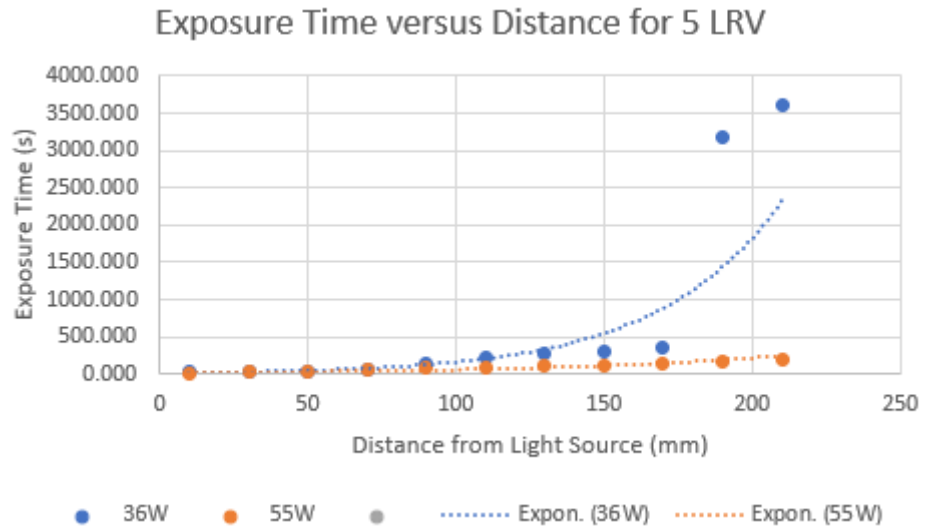


Figure 4.96: Total Required Exposure Time Required to Reach 5 LRV for Angled Configuration

Based on results, the exposure time required to reach the total dose increased as the distance of sensor from the light source increased. It can be concluded that the efficiency of UV-C light decreases as the distance from the light source increases due to the irradiation profile drops across distance, meaning that the surface requires more time to receive the same amount of UV energy as the distance from the light source increases. The results also show that the total exposure time required to reach a specific UV dose varies depending on the power of the light source. At a far distance of around 170 mm, the trend of total exposure time increased dramatically for the 36 W light source, while it increased gradually for the 55 W light source. This indicates that higher power light sources are more efficient at delivering UV energy over longer distances.

Table 4.9 to 4.12 provide a summary of the results based on the optical simulation, which can be useful for understanding the efficiency of UVGI at different distances and power levels for both configurations. In short, it is important to consider both the distance and power of the UV-C light source when determining the appropriate exposure time required for effective disinfection.

Table 4.9: Summary of Total Exposure Time Required to Reach Respective LRV for 36W Vertical Configuration

Power Source = 36W @ Vertical Configuration											
Distance From Light Source (mm)	10	30	50	70	90	110	130	150	170	190	210
Total Time Exposure Required for LRV 3 (s)	1.001	1.674	2.372	4.038	6.936	7.731	8.088	8.809	12.737	39.973	60.997
Total Time Exposure Required for LRV 4 (s)	4.868	8.138	11.536	19.637	33.730	37.594	39.329	42.836	61.935	194.378	296.613
Total Time Exposure Required for LRV 5 (s)	16.599	27.753	39.339	66.966	115.023	128.199	134.117	146.076	211.206	662.850	1011.481

Table 4.10: Summary of Total Exposure Time Required to Reach Respective LRV for 55W Vertical Configuration

Power Source = 55W @ Vertical Configuration											
Distance From Light Source (mm)	10	30	50	70	90	110	130	150	170	190	210
Total Time Exposure Required for LRV 3 (s)	0.550	0.960	1.365	2.273	3.034	3.741	4.289	5.004	7.279	8.070	9.098
Total Time Exposure Required for LRV 4 (s)	2.675	4.667	6.637	11.051	14.752	18.194	20.858	24.332	35.395	39.242	44.243
Total Time Exposure Required for LRV 5 (s)	9.121	15.915	22.634	37.686	50.305	62.042	71.129	82.974	120.699	133.818	150.874

Table 4.11: Summary of Total Exposure Time Required to Reach
Respective LRV for 36W Angled Configuration

Power Source = 36W @ Angled Configuration											
Distance From Light Source (mm)	10	30	50	70	90	110	130	150	170	190	210
Total Time Exposure Required for LRV 3 (s)	1.399	2.169	2.897	4.301	8.472	13.401	17.056	18.921	22.280	191.881	217.345
Total Time Exposure Required for LRV 4 (s)	6.804	10.547	14.089	20.915	41.196	65.164	82.940	92.008	108.342	933.064	1056.889
Total Time Exposure Required for LRV 5 (s)	23.204	35.967	48.044	71.323	140.482	222.217	282.835	313.755	369.458	3181.842	3604.098

Table 4.12: Summary of Total Exposure Time Required to Reach
Respective LRV for 36W Angled Configuration

Power Source = 55W @ Vertical Configuration											
Distance From Light Source (mm)	10	30	50	70	90	110	130	150	170	190	210
Total Time Exposure Required for LRV 3 (s)	0.641	1.460	2.105	2.976	4.586	5.334	6.370	7.729	8.671	9.657	11.239
Total Time Exposure Required for LRV 4 (s)	3.119	7.097	10.236	14.471	22.301	25.940	30.978	37.585	42.163	46.960	54.654
Total Time Exposure Required for LRV 5 (s)	10.635	24.203	34.905	49.348	76.048	88.457	105.638	128.167	143.779	160.139	186.376

CHAPTER 5

CONCLUSIONS

5.1 Summary

The goal of this project is to evaluate the efficiency of UV-C light for different combinations of distance and radiation intensity at a spectrum of 254 nm via optical simulation approach. In the case study, the total dose required to inactivate SARS-Cov-2 at 3,4 and 5 log reduction value are determined as 6.556 mW/cm^2 , 31.880 mW/cm^2 and 108.714 mW/cm^2 . The irradiation profile of the UV-C light was generated through ANSYS SPEOS optical simulation software, with varying power levels of 36 W and 55 W at distances ranging from 10 mm to 210 mm. Based on the data, the results indicated that the efficiency of UVGI increased at a higher power level of 55 W and at a shorter distance from the surface being disinfected at 10 mm.

Although the project has a successful outcome, there is still plenty of improvement that could be done in the future. One of the improvements that can be implemented are conducting a more advanced optical simulation that consider the effects of contaminants either in the environment or on the surface of the light bulb. This would allow for a more accurate determination of the efficiency of surface disinfection in environments with varying degrees of turbidity. This information is valuable to be used to predict the

effectiveness and optimal usage of UVGI systems in areas with high levels of turbidity.

As direct UVGI method possesses a limitation on indirect surface such as the surface behind an object, certain studies recommend incorporating reflective surface, such as mirrors or reflective paint, to increase the efficiency of surface disinfection on these indirect surfaces. As part of future work, an optical simulation could be conducted that includes reflective surfaces, which would enable the prediction of surface disinfection performance on indirect surfaces.

In short, the experiments and simulations conducted in this study demonstrate that both the distance and power of the UV-C light source have a significant impact on the effectiveness of surface disinfection. By measuring and controlling the UV dose, it is possible to ensure that the UVGI system is delivering an effective level of disinfection in different case.

REFERENCES

- [1] A. Rutala, W. and J. Weber, D., 2008. Guideline for Disinfection and Sterilization in Healthcare Facilities, 2008. [online] Available at: <<https://www.cdc.gov/infectioncontrol/pdf/guidelines/disinfection-guidelines-H.pdf>> [Accessed 9 July 2022].
- [2] Armellino, D. et al. (2019) “Assessment of focused multi vector ultraviolet disinfection with shadowless delivery using 5-point multisided sampling of patient care equipment without manual-chemical disinfection,” *American Journal of Infection Control*, 47(4), pp. 409–414. Available at: <https://doi.org/10.1016/j.ajic.2018.09.019>.
- [3] Artasensi, A., Mazzotta, S. and Fumagalli, L., 2021. Back to Basics: Choosing the Appropriate Surface Disinfectant. *Antibiotics*, 10(6), p.613.
- [4] Beal, A. et al. (2016) “First UK trial of Xenex PX-UV, an automated ultraviolet room decontamination device in a clinical haematology and Bone Marrow Transplantation Unit,” *Journal of Hospital Infection*, 93(2), pp. 164–168. Available at: <https://doi.org/10.1016/j.jhin.2016.03.016>.
- [5] Bergman, R., 2021. Germicidal UV Sources and Systems †. *Photochemistry and Photobiology*, 97(3), pp.466-470.
- [6] Bernard, J.E. and Morgan, H. (1904) “Upon the bactericidal action of some ultra-violet radiations as produced by the continuous-current arc,” *Proceedings of the Royal Society of London*, 72(477-486), pp. 126–128. Available at: <https://doi.org/10.1098/rspl.1903.0028>.
- [7] Beukers, R. and Berends, W. (1960) “Isolation and identification of the irradiation product of thymine,” *Biochimica et Biophysica Acta*, 41(3), pp. 550–551. Available at: [https://doi.org/10.1016/0006-3002\(60\)90063-9](https://doi.org/10.1016/0006-3002(60)90063-9).
- [8] Byrns, G. et al. (2017) “The uses and limitations of a hand-held germicidal ultraviolet wand for surface disinfection,” *Journal of Occupational and Environmental Hygiene*, 14(10), pp. 749–757. Available at: <https://doi.org/10.1080/15459624.2017.1328106>.
- [9] Caballero, S. et al. (2004) “Rotavirus virus-like particles as surrogates in environmental persistence and inactivation studies,” *Applied and Environmental Microbiology*, 70(7), pp. 3904–3909. Available at: <https://doi.org/10.1128/aem.70.7.3904-3909.2004>.

- [10] Cai, S., Zuo, C., Zhang, J., Liu, H. and Fang, X., 2021. A Paper-Based Wearable Photodetector for Simultaneous UV Intensity and Dosage Measurement. *Advanced Functional Materials*, 31(20), p.2100026.
- [11] Chen, L.-hua et al. (2020) “Evaluation of a pulsed xenon ultraviolet light device for reduction of pathogens with biofilm-forming ability and impact on environmental bioburden in Clinical Laboratories,” *Photodiagnosis and Photodynamic Therapy*, 29, p. 101544. Available at: <https://doi.org/10.1016/j.pdpdt.2019.08.026>.
- [12] Cleaning and Disinfecting Transit Vehicles and Facilities During a Contagious Virus Pandemic (2021). American Public Transportation Association. Available at: <https://www.apta.com/research-technical-resources/standards/security/apta-ss-iss-wp-001-20/> (Accessed: December 1, 2022).
- [13] Coohill, T.P. (1997) “Historical aspects of ultraviolet action spectroscopy*,” *Photochemistry and Photobiology*, 65(s1). Available at: <https://doi.org/10.1111/j.1751-1097.1997.tb07974.x>.
- [14] Cutler, T.D. and Zimmerman, J.J. (2011) “Ultraviolet irradiation and the mechanisms underlying its inactivation of infectious agents,” *Animal Health Research Reviews*, 12(1), pp. 15–23. Available at: <https://doi.org/10.1017/s1466252311000016>.
- [15] Derraik, J.G. et al. (2020) “Rapid review of SARS-COV-1 and SARS-COV-2 viability, susceptibility to treatment, and the disinfection and reuse of PPE, particularly filtering facepiece respirators,” *International Journal of Environmental Research and Public Health*, 17(17), p. 6117. Available at: <https://doi.org/10.3390/ijerph17176117>.
- [16] Detection and Enumeration of Bacteria in Swabs and Other Environmental Samples (2017). Public Health England. Available at: https://assets.publishing.service.gov.uk/government/uploads/system/uploads/attachment_data/file/660648/Detection_and_enumeration_of_bacteria_in_swabs_and_other_environmental_samples.pdf (Accessed: December 1, 2022).
- [17] Dexter, F., Birchansky, B., Epstein, R. and Loftus, R., 2022. Average and longest expected treatment times for ultraviolet light disinfection of rooms. *American Journal of Infection Control*, 50(1), pp.61-66.
- [18] Downes, A. AND Blunt, T.P. (1877) “The influence of light upon the development of bacteria 1,” *Nature*, 16(402), pp. 218–218. Available at: <https://doi.org/10.1038/016218a0>.
- [19] Downes, A. AND Blunt, T.P. (1879) “Iv. on the influence of light upon protoplasm,” *Proceedings of the Royal Society of London*, 28(190-195), pp. 199–212. Available at: <https://doi.org/10.1098/rspl.1878.0109>.

- [20] El Haddad, L. et al. (2017) "Evaluation of a pulsed xenon ultraviolet disinfection system to decrease bacterial contamination in operating rooms," *BMC Infectious Diseases*, 17(1). Available at: <https://doi.org/10.1186/s12879-017-2792-z>.
- [21] Elgужja, A., Altalhi, H. and Ezreqat, S., 2019. Review of the Efficacy of UVC for Surface Decontamination.
- [22] Enwemeka, C.S., Baker, T.L. and Bumah, V.V. (2021) "The role of UV and blue light in photo-eradication of Microorganisms," *Journal of Photochemistry and Photobiology*, 8, p. 100064. Available at: <https://doi.org/10.1016/j.jpap.2021.100064>.
- [23] Forges, M., Bardin, M., Urban, L., Aarouf, J. and Charles, F., 2020. Impact of UV-C Radiation Applied during Plant Growth on Pre- and Postharvest Disease Sensitivity and Fruit Quality of Strawberry. *Plant Disease*, 104(12), pp.3239-3247.
- [24] Fredes, P. et al. (2021) "Estimation of the ultraviolet-C doses from mercury lamps and light-emitting diodes required to disinfect surfaces," *Journal of Research of the National Institute of Standards and Technology*, 126. Available at: <https://doi.org/10.6028/jres.126.025>.
- [25] Freeman, S. et al. (2022) "Systematic evaluating and modeling of SARS-COV-2 UVC disinfection," *Scientific Reports*, 12(1). Available at: <https://doi.org/10.1038/s41598-022-09930-2>.
- [26] Gates, F.L. (1929) "A study of the bactericidal action of Ultra Violet Light," *Journal of General Physiology*, 13(2), pp. 231–248. Available at: <https://doi.org/10.1085/jgp.13.2.231>.
- [27] Gates, F.L. (1929) "A study of the bactericidal action of Ultra Violet Light," *Journal of General Physiology*, 13(2), pp. 249–260. Available at: <https://doi.org/10.1085/jgp.13.2.249>.
- [28] Gates, F.L. (1930) "A study of the bactericidal action of Ultra Violet Light," *Journal of General Physiology*, 14(1), pp. 31–42. Available at: <https://doi.org/10.1085/jgp.14.1.31>.
- [29] Gayas, B., Munaza, B. and Sidhu, G.K. (2019) "Ultraviolet light treatment of fresh fruits and vegetables," *Processing of Fruits and Vegetables*, pp. 83–100. Available at: <https://doi.org/10.1201/9780429505775-7>.
- [30] Gerba, C.P., Gramos, D.M. and Nwachuku, N. (2002) "Comparative inactivation of enteroviruses and adenovirus 2 by UV light," *Applied and Environmental Microbiology*, 68(10), pp. 5167–5169. Available at: <https://doi.org/10.1128/aem.68.10.5167-5169.2002>.

- [31] Ghedini, E., Pizzolato, M., Longo, L., Menegazzo, F., Zanardo, D. and Signoreto, M., 2021. Which Are the Main Surface Disinfection Approaches at the Time of SARS-CoV-2?. *Frontiers in Chemical Engineering*, 2.
- [32] Gidari, A. et al. (2021) “SARS-COV-2 survival on surfaces and the effect of UV-C light,” *Viruses*, 13(3), p. 408. Available at: <https://doi.org/10.3390/v13030408>.
- [33] Gilkeson, C.A. and Noakes, C. (2012) “Application of CFD simulation to predicting upper-room uvgi effectiveness,” *Photochemistry and Photobiology*, 89(4), pp. 799–810. Available at: <https://doi.org/10.1111/php.12013>.
- [34] Hockberger, P.E. (2007) “A history of ultraviolet photobiology for humans, animals and microorganisms,” *Photochemistry and Photobiology*, 76(6), pp. 561–579. Available at: [https://doi.org/10.1562/0031-8655\(2002\)0760561ahoupf2.0.co2](https://doi.org/10.1562/0031-8655(2002)0760561ahoupf2.0.co2).
- [35] Jaszczak, M., Sasiadek-Andrzejczak, E. and Kozicki, M., 2022. Discolouring 3D Gel Dosimeter for UV Dose Distribution Measurements. *Materials*, 15(7), p.2546.
- [36] Hou, M., Pantelic, J. and Aviv, D. (2021) “Spatial analysis of the impact of UVGI technology in occupied rooms using Ray-Tracing Simulation,” *Indoor Air*, 31(5), pp. 1625–1638. Available at: <https://doi.org/10.1111/ina.12827>.
- [37] Husman, A.M. et al. (2004) “Calicivirus inactivation by nonionizing (253.7-nanometer-wavelength [UV]) and ionizing (gamma) radiation,” *Applied and Environmental Microbiology*, 70(9), pp. 5089–5093. Available at: <https://doi.org/10.1128/aem.70.9.5089-5093.2004>.
- [38] Ilt5000 lab radiometer for broadband germicidal and UV hazard measurements (no date) Ilt5000, SED240/ACT5/W | Germicidal & UV Disinfection. Available at: <https://internationallight.com/products/ilt5000-lab-radiometer-broadband-germicidal-and-uv-hazard-measurements> (Accessed: February 27, 2023).
- [39] Jinadatha, C. et al. (2015) “Is the pulsed xenon ultraviolet light no-touch disinfection system effective on methicillin-resistant *Staphylococcus aureus* in the absence of manual cleaning?,” *American Journal of Infection Control*, 43(8), pp. 878–881. Available at: <https://doi.org/10.1016/j.ajic.2015.04.005>.
- [40] Jones, Daniel & Ivanovich, Michael. (2020). UV-C for HVAC Air and Surface Disinfection. 2-11.

- [41] Kennedy, H.E. (2019) 2019 Ashrae handbook: Heating, ventilating, and air-conditioning applications. Atlanta, GA: American Society of Heating, Refrigerating and Air-Conditioning Engineers.
- [42] Klein, J.E. (2002) “Demystifying the sequential ray-tracing algorithm,” SPIE Proceedings [Preprint]. Available at: <https://doi.org/10.1117/12.481191>.
- [43] Kohli, I. et al. (2019) “Impact of long-wavelength ultraviolet A1 and visible light on light-skinned individuals,” *Photochemistry and Photobiology*, 95(6), pp. 1285–1287. Available at: <https://doi.org/10.1111/php.13143>.
- [44] Kowalski, W. (2009) “Ultraviolet germicidal irradiation handbook.” Available at: <https://doi.org/10.1007/978-3-642-01999-9>.
- [45] Lau, J., Bahnfleth, W. and Freihaut, J. (2009) “Estimating the effects of ambient conditions on the performance of UVGI Air Cleaners,” *Building and Environment*, 44(7), pp. 1362–1370. Available at: <https://doi.org/10.1016/j.buildenv.2008.05.015>.
- [46] Lidwell, O.M. and Lowbury, E.J. (1950) “The survival of bacteria in dust. II. the effect of atmospheric humidity on the survival of bacteria in dust,” *Journal of Hygiene*, 48(1), pp. 21–27. Available at: <https://doi.org/10.1017/s0022172400014868>.
- [47] Lindblad, M., Tano, E., Lindahl, C. and Huss, F., 2020. Ultraviolet-C decontamination of a hospital room: Amount of UV light needed. *Burns*, 46(4), pp.842-849.
- [48] Lindsley, W.G. et al. (2017) “Ambulance disinfection using ultraviolet germicidal irradiation (UVGI): Effects of fixture location and surface reflectivity,” *Journal of Occupational and Environmental Hygiene*, 15(1), pp. 1–12. Available at: <https://doi.org/10.1080/15459624.2017.1376067>.
- [49] Lindsley, W.G. et al. (2015) “Effects of ultraviolet germicidal irradiation (UVGI) on N95 respirator filtration performance and structural integrity,” *Journal of Occupational and Environmental Hygiene*, 12(8), pp. 509–517. Available at: <https://doi.org/10.1080/15459624.2015.1018518>.
- [50] Ling, J., Zhang, X., Zheng, W. and Xing, J., 2018. Evaluation of biological inactivation efficacy for in-duct pulsed xenon lamp. *Building and Environment*, 143, pp.178-185.
- [51] Luo, H. and Zhong, L. (2021) “Ultraviolet germicidal irradiation (UVGI) for in-duct airborne bioaerosol disinfection: Review and analysis of Design Factors,” *Building and Environment*, 197, p. 107852. Available at: <https://doi.org/10.1016/j.buildenv.2021.107852>.

- [52] Ma, B. et al. (2021) “UV inactivation of SARS-COV-2 across the UVC spectrum: KrCl* excimer, mercury-vapor, and light-emitting-diode (LED) sources,” *Applied and Environmental Microbiology*, 87(22). Available at: <https://doi.org/10.1128/aem.01532-21>.
- [53] Mallikarjuna, K. et al. (2016) “Photonic welding of ultra-long copper nanowire network for flexible transparent electrodes using white flash light sintering,” *RSC Advances*, 6(6), pp. 4770–4779. Available at: <https://doi.org/10.1039/c5ra25548a>.
- [54] Masse, V. et al. (2018) “Comparing and optimizing ultraviolet germicidal irradiation systems use for patient room terminal disinfection: An exploratory study using radiometry and commercial test cards,” *Antimicrobial Resistance & Infection Control*, 7(1). Available at: <https://doi.org/10.1186/s13756-018-0317-1>.
- [55] McGinn, C. et al. (2021) “Exploring the applicability of robot-assisted UV disinfection in Radiology,” *Frontiers in Robotics and AI*, 7. Available at: <https://doi.org/10.3389/frobt.2020.590306>.
- [56] Memarzadeh, F. (2021) “A review of recent evidence for utilizing ultraviolet irradiation technology to disinfect both indoor air and surfaces,” *Applied Biosafety*, 26(1), pp. 52–56. Available at: <https://doi.org/10.1089/apb.20.0056>.
- [57] Mkabela, M. (2021) in Radiometric germicidal effectiveness and safety of commercial UV germicidal irradiance (UVGI) devices.
- [58] Mohamadi, F. and Fazeli, A., 2022. A Review on Applications of CFD Modeling in COVID-19 Pandemic. *Archives of Computational Methods in Engineering*,.
- [59] Molitor, R. et al. (2020) “Agar plate-based screening methods for the identification of polyester hydrolysis by *Pseudomonas* species,” *Microbial Biotechnology*, 13(1), pp. 274–284. Available at: <https://doi.org/10.1111/1751-7915.13418>.
- [60] Morikane, K. et al. (2020) “Clinical and microbiological effect of pulsed xenon ultraviolet disinfection to reduce multidrug-resistant organisms in the intensive care unit in a Japanese hospital: A before-after study,” *BMC Infectious Diseases*, 20(1). Available at: <https://doi.org/10.1186/s12879-020-4805-6>.
- [61] O'Connor, C., Courtney, C. and Murphy, M. (2020) “Shedding light on the myths of ultraviolet radiation in the COVID-19 pandemic,” *Clinical and Experimental Dermatology*, 46(1), pp. 187–188. Available at: <https://doi.org/10.1111/ced.14456>.

- [62] Palakornkitti, P. et al. (2021) “The effectiveness of commercial household ultraviolet C germicidal devices in Thailand,” *Scientific Reports*, 11(1). Available at: <https://doi.org/10.1038/s41598-021-03326-4>.
- [63] Philips (1985) *UVGI Catalog and Design Guide*. Catalog NO. U.D.C.628.9, Netherlands.
- [64] Pravda, J., 2020. Hydrogen peroxide and disease: towards a unified system of pathogenesis and therapeutics. *Molecular Medicine*, 26(1).
- [65] Public Transport Authorities And COVID-19 (2020). International Association of Public Transport. Available at: <https://www.lek.com/sites/default/files/PDFs/COVID19-public-transport-impacts.pdf/> (Accessed: December 1, 2022).
- [66] Raggi, R. et al. (2018) “Clinical, operational, and financial impact of an ultraviolet-C terminal disinfection intervention at a community hospital,” *American Journal of Infection Control*, 46(11), pp. 1224–1229. Available at: <https://doi.org/10.1016/j.ajic.2018.05.012>.
- [67] Rutala, W.A., Gergen, M.F. and Weber, D.J. (2010) “Room decontamination with UV radiation,” *Infection Control & Hospital Epidemiology*, 31(10), pp. 1025–1029. Available at: <https://doi.org/10.1086/656244>.
- [68] Sabino, C.P. et al. (2020) “UV-C (254 nm) lethal doses for SARS-COV-2,” *Photodiagnosis and Photodynamic Therapy*, 32, p. 101995. Available at: <https://doi.org/10.1016/j.pdpdt.2020.101995>.
- [69] Sanchez, A.G. and Smart, W.D. (2022) “Verifiable surface disinfection using ultraviolet light with a mobile manipulation robot,” *Technologies*, 10(2), p. 48. Available at: <https://doi.org/10.3390/technologies10020048>.
- [70] Scott, R., Joshi, L.T. and McGinn, C. (2022) “Hospital surface disinfection using ultraviolet germicidal irradiation technology: A Review,” *Healthcare Technology Letters*, 9(3), pp. 25–33. Available at: <https://doi.org/10.1049/htl2.12032>.
- [71] Sholtes, K.A. et al. (2016) “Comparison of ultraviolet light-emitting diodes and low-pressure mercury-arc lamps for disinfection of water,” *Environmental Technology*, 37(17), pp. 2183–2188. Available at: <https://doi.org/10.1080/09593330.2016.1144798>.
- [72] Song, K., Taghipour, F. and Mohseni, M. (2019) “Microorganisms inactivation by wavelength combinations of ultraviolet light-emitting diodes (UV-leds),” *Science of The Total Environment*, 665, pp. 1103–1110. Available at: <https://doi.org/10.1016/j.scitotenv.2019.02.041>.

- [73] Song, L. et al. (2020) “Development of a pulsed xenon ultraviolet disinfection device for real-time air disinfection in ambulances,” *Journal of Healthcare Engineering*, 2020, pp. 1–5. Available at: <https://doi.org/10.1155/2020/6053065>.
- [74] Tande, B., Pringle, T., Rutala, W., Gergen, M. and Weber, D., 2018. Understanding the effect of ultraviolet light intensity on disinfection performance through the use of ultraviolet measurements and simulation. *Infection Control & Hospital Epidemiology*, 39(9), pp.1122-1124.
- [75] Tanner, B. (2015) Log and percent reductions in microbiology and antimicrobial testing, Microchem Laboratory. Available at: <https://microchemlab.com/information/log-and-percent-reductions-microbiology-and-antimicrobial-testing/> (Accessed: February 28, 2023).
- [76] Thom, K.A. et al. (2012) “Comparison of swab and sponge methodologies for identification of *Acinetobacter baumannii* from the hospital environment,” *Journal of Clinical Microbiology*, 50(6), pp. 2140–2141. Available at: <https://doi.org/10.1128/jcm.00448-12>.
- [77] Thompson, S.S. et al. (2003) “Detection of infectious human adenoviruses in tertiary-treated and ultraviolet-disinfected wastewater,” *Water Environment Research*, 75(2), pp. 163–170. Available at: <https://doi.org/10.2175/106143003x140944>.
- [78] Thurston-Enriquez, J.A. et al. (2003) “Inactivation of feline calicivirus and adenovirus type 40 by UV radiation,” *Applied and Environmental Microbiology*, 69(1), pp. 577–582. Available at: <https://doi.org/10.1128/aem.69.1.577-582.2003>.
- [79] TUV PL-L (2022) Philips. Available at: <https://www.lighting.philips.com.my/prof/conventional-lamps-and-tubes/special-lamps/purificationwater-and-air/air/tuv-pl-l> (Accessed: February 19, 2023).
- [80] Tyndall, J. (1879) “V. note on the influence exercised by light on organic infusions,” *Proceedings of the Royal Society of London*, 28(190-195), pp. 212–213. Available at: <https://doi.org/10.1098/rspl.1878.0110>.
- [81] Tyndall, J. (1881) “On the arrestation of infusorial life,” *Science*, os-2(68), pp. 478–478. Available at: <https://doi.org/10.1126/science.os-2.68.478>.
- [82] Vanhaelewyn, L., Van Der Straeten, D., De Coninck, B. and Vandebussche, F., 2020. Ultraviolet Radiation From a Plant Perspective: The Plant-Microorganism Context. *Frontiers in Plant Science*, 11.

- [83] VAZIRI, N., 2018. Low pressure mercury–argon electrodeless fluorescent lamp simulation using the finite volume method. *Plasma Science and Technology*, 20(10), p.105403.
- [84] Walton, A.C. (1916) “Reactions of paramoecium caudatum to light.,” *Journal of Animal Behavior*, 6(5), pp. 335–340. Available at: <https://doi.org/10.1037/h0070032>.
- [85] Wan Yunoh, W.S. et al. (2021) “A study on UVC irradiance emitted by various types of UVGI products,” *IOP Conference Series: Materials Science and Engineering*, 1106(1), p. 012008. Available at: <https://doi.org/10.1088/1757-899x/1106/1/012008>.
- [86] Wiwanitkit, V. (2017) “Finite-difference time-domain method application in nanomedicine,” *Computational Nanotechnology Using Finite Difference Time Domain*, pp. 291–328. Available at: <https://doi.org/10.1201/b16319-7>.
- [87] Wladyslaw, J.K. (2021) “Ultraviolet Germicidal Irradiation for Air and Surface Disinfection of Animal Facilities,”. Available at: <https://doi.org/10.13140/RG.2.2.25472.15361>
- [88] Yamano, N., Kunisada, M., Kaidzu, S., Sugihara, K., Nishiaki-Sawada, A., Ohashi, H., Yoshioka, A., Igarashi, T., Ohira, A., Tanito, M. and Nishigori, C., 2020. Long-term Effects of 222-nm ultraviolet radiation C Sterilizing Lamps on Mice Susceptible to Ultraviolet Radiation. *Photochemistry and Photobiology*, 96(4), pp.853-862..
- [89] Yang, J.-H. et al. (2019) “Effectiveness of an ultraviolet-C disinfection system for reduction of healthcare-associated pathogens,” *Journal of Microbiology, Immunology and Infection*, 52(3), pp. 487–493. Available at: <https://doi.org/10.1016/j.jmii.2017.08.017>.
- [90] Yemmireddy, V., Adhikari, A. and Moreira, J. (2022) “Effect of ultraviolet light treatment on microbiological safety and quality of fresh produce: An overview,” *Frontiers in Nutrition*, 9. Available at: <https://doi.org/10.3389/fnut.2022.871243>.
- [91] Zakaria, F., Harelimana, B., Čurko, J., van de Vossenbergh, J., Garcia, H., Hooijmans, C. and Brdjanovic, D., 2016. Effectiveness of UV-C light irradiation on disinfection of an eSOS® smart toilet evaluated in a temporary settlement in the Philippines. *International Journal of Environmental Health Research*, 26(5-6), pp.536-553.
- [92] Zhang, H. et al. (2020) “Disinfection by in-duct ultraviolet lamps under different environmental conditions in turbulent airflows,” *Indoor Air*, 30(3), pp. 500–511. Available at: <https://doi.org/10.1111/ina.12642>.

- [93] Zou, Y., Zhao, X. and Chen, Q., 2017. Comparison of STAR-CCM+ and ANSYS Fluent for simulating indoor airflows. *Building Simulation*, 11(1), pp.165-174.

APPENDICES